This is a post-peer-review, pre-copyedit version of an article published in the Journal Construction and Building Materials. The final authenticated version is available online at: https://doi.org/10.1016/j.conbuildmat.2022.128041

An Aggregated Non-destructive Testing (NDT) Framework for the Assessment of Mechanical Properties of Unreinforced Masonry Italian Medieval Churches

David Pirchio[a,b]*, Kevin Q. Walsh[a,b], Elizabeth Kerr[a], Ivan Giongo[c], Marta Giaretton[d], Brad D. Weldon[a,b], Luca Ciocci[e], and Luigi Sorrentino[f]

[a]Department of Civil and Environmental Engineering & Earth Sciences, University of Notre Dame, South Bend, Indiana, USA; [b]Frost Engineering & Consulting, Mishawaka, Indiana, USA; [c]Department of Civil, Environmental and Mechanical Engineering, University of Trento, Trento, Italy; [d]Dizhur Consulting, Auckland, New Zealand; [e]Office for Cultural Heritage and Religious Buildings of the Diocese of Anagni-Alatri, Italy; [f]Department of Structural and Geotechnical Engineering, Sapienza University of Rome, Roma, Italy.

*e-mail: dpirchio@nd.edu; mail: Department of Civil and Environmental Engineering & Earth Sciences, University of Notre Dame, 156 Fitzpatrick Hall of Engineering, Notre Dame, IN 46556, USA

Abstract

Medieval churches constructed of unreinforced masonry (URM) represent critical assets of Italian architectural heritage. In order to preserve these churches against earthquakes, obtaining robust information regarding their material mechanical characteristics is necessary as part of a reliable structural analysis and strengthening intervention. Given the drawbacks of semi-destructive or destructive testing of heritage material, non-destructive testing (NDT) is the most viable approach to obtain data regarding the mechanical characteristics of the material composing the structure of the churches. However, there are several uncertainties inherent within NDT techniques based on the current state of the art. Thus, two different NDT techniques (i.e., rebound hammer testing, and pulse velocity testing) and two expert judgment-based investigation techniques (i.e., masonry quality index, and mechanical properties ranges based on the Commentary to the Italian building code) were applied to 170 specimens belonging to the walls of 72 URM Italian medieval churches to assess the quality of the URM and its components. The surveyed churches walls, although highly variable in geometry, materials, and conditions, can be sorted in four URM types: a) irregular stone masonry, with pebbles, erratic and irregular stone units; b) roughly cut stone with good bond; c) ashlar masonry with regular squared blocks and mortar joints; and d) solid fired clay bricks with lime mortar. Subsequently, using the SonReb approach, predictive equations that aggregate the two NDT techniques, and the correlation coefficient specific for each URM type were developed to define some of the critical mechanical properties of the URM (i.e., compressive strength, Young's modulus, and shear modulus). The mechanical properties determined via predictive equations were then plotted and compared with the predictions of the two well-established expert judgment-based investigation techniques to evaluate the accuracy of the approach. Finally, a partial validation based on NDT and destructive testing techniques of six URM prisms was performed to evaluate the accuracy of the proposed predictive equations. Ultimately, three equations to determine the compressive strength, the Young's modulus, and the shear modulus were developed. The developed equations offer to engineering practitioners a rapid and NDT technique to assess URM properties that would not solely rely on the judgment and expertise of the surveyor.

Keywords: medieval churches; URM buildings; non-destructive testing (NDT) techniques; masonry types; masonry mechanical properties; *MQI*; rebound hammer testing; pulse velocity testing; SonReb technique.

List of Notations

URM is the abbreviation for "unreinforced masonry";

NDT is the abbreviation for "non-destructive testing";

MQI is the abbreviation for "masonry quality index";

f'_m is the URM compressive strength (MPa);

E_m is the URM Young's modulus (MPa);

E_{dm} is the URM dynamic modulus of elasticity (MPa);

G_m is the URM shear modulus (MPa);

w is the URM specific weight (kN/m^3);

ν is the URM Poisson's ratio;

g is the gravitational acceleration (m/s^2);

R is the rebound number; and

v_i is the indirect pulse velocity (m/s).

1. Introduction

Unreinforced masonry (URM) has been the most largely utilized construction material in Italy since the early major civilizations (e.g., Etruscan and Roman) and remained so until the introduction of reinforced concrete in the late 1800s [1, 2, 3, 4]. Furthermore, given the durability of masonry, most of the historic structures still in existence are partially or totally composed of URM. The High and Late Middle Ages represent periods of intense masonry construction during which a large proportion of Italian architectural heritage was built [5]. Some examples of the prototypical considered churches considered in the current study are shown in Figure 1.

Figure 1 – Prototypical examples of churches surveyed: a) Santa Maria Assunta (Dasindo, Trentino – Alto Adige); b) San Matteo Apostolo (Cavazzale, Veneto); c) Santi Leonardo e Cristoforo (Monticchiello, Toscana); d) Sant'Ansano Martire (Petrignano del Lago, Umbria); e) Maddalena (Alatri, Lazio); f) Santa Maria di Casarlano (Casarlano, Campania).

Given the cultural importance of URM medieval churches, and the vulnerability of this construction type observed in past earthquakes, such as in Friuli-Venezia Giulia in 1976 [6], in Basilicata and Campania in 1980 [7], in Umbria-Marche in 1997 [8, 9], in Molise in 2002 [10], in L'Aquila in 2009 [11, 12], in Emilia in 2012 [13], and in central Italy in 2016 [14], a holistic risk assessment methodology to justify the decision-making process of the dioceses concerning the retrofitting interventions was developed [15]. In regard to improving the risk assessment methodology, and as a basis for further studies, a more sophisticated analysis regarding the mechanical material properties of the considered churches was conducted as reported herein.

While boundary conditions and component geometry (e.g., wall height-to-thickness ratio) are the dominating variables for the out-of-plane behavior of URM structures [16, 17, 18], material mechanical properties (e.g., masonry compressive strength, elastic modulus, and shear strength) often govern the in-plane and the dynamic behavior of URM structures [16, 19, 20]. The determination of the mechanical properties – especially in historic buildings with non-homogeneous construction due to additions and reparations over time – is process-dependent on the adopted assessing technique, especially when non-destructive testing (NDT) techniques are applied, which are generally and inherently less precise and less accurate than destructive and semi-destructive techniques [21]. Nonetheless, the current research was targeted to the development of a dependable NDT assessment methodology for three primary reasons:

- Historic buildings are often subject to regulatory and artistic constraints that prohibit the extraction of specimens to be studied in laboratory testing using destructive techniques unless a strengthening intervention is in progress;
- NDT techniques are generally more rapid and less cost-demanding than semi-destructive and destructive techniques, and hence more suitable for use in a time-efficient risk assessment methodology [15]; and
- Although several studies have been conducted using different NDT techniques on masonry buildings (e.g., [22, 23, 24, 25, 26]), the authors are aware of only limited research in which the discrepancies amongst different NDT techniques are considered (e.g., [27, 28, 29, 30]) and mostly with respect to the components (i.e., bricks and mortar) rather than the URM as a composite material.

While visual assessing procedures to estimate URM mechanical properties are acknowledged by the Italian Code for Construction (MIT 2018) [31] and its commentary (MIT 2019) [32] – such as the masonry quality index (MQI) [33, 34] and the URM type mechanical properties ranges provided by the MIT 2019 [32] – the outcome of such procedures is largely dependent on the judgment and expertise of the surveyor. While quantitative NDT techniques based on in-situ testing are available (e.g., [26]), they are generally limited to the scope of assessing the properties of the URM components (i.e., either the units or the mortar). Given the importance of assessing rapidly a large number of URM historic buildings, and limiting the cost and time required for such investigations, the authors' goal was to develop a novel method that combined multiple NDT techniques into a comprehensive tool for practitioners to cost-efficiently assess the URM properties without relying on visual and subjective judgment.

The proposed aggregated procedure was developed as a combination of the rebound hammer testing and the pulse velocity testing following the SonReb approach [35, 36, 37]. Given that no sample extraction of the tested URM walls was allowed (per owners' request and given the heritage nature of the buildings), two existing and well-established expert judgment-based investigation procedures (i.e. MQI, and URM type mechanical properties ranges provided by the MIT 2019 [32]) were still used for the calibration of the correlation coefficients of the proposed predictive equations. The accuracy of such calibration was partially validated by re-applying the method on a different (and more modern) URM building from which URM samples could be extracted and destructively tested in laboratory. While the current research aims to prove the usefulness and validity of the proposed aggregated technique, the authors encourage further research on the topic for a better calibration of the proposed predictive equations via extensive destructive testing comparison.

The authors acknowledge that any NDT technique, including the proposed aggregated framework, is inherently less accurate than both destructive and semi-destructive techniques, however, there are several cases where for a level 1 type of assessment [38], more in depth material properties assessment techniques are too time-consuming, costly, and incompatible with listed constructions. Furthermore, even minor destructive testing (MDT) techniques (e.g., pull-out method, Windsor-Probe method, and pull-off method) could be restricted, as in the specific case of the current research, as the owner would not allow any sort of damage to the building. Given the premises, the authors advise the use of the herein proposed aggregated NDT method in all those cases in which a rapid and objective evaluation of the URM mechanical properties for a level 1 type of assessment [38] is required, no sort of damage to the building nor samples extraction from the URM is allowed, and some degree of uncertainty is considered acceptable.

2. Churches, Macro-blocks, and Materials

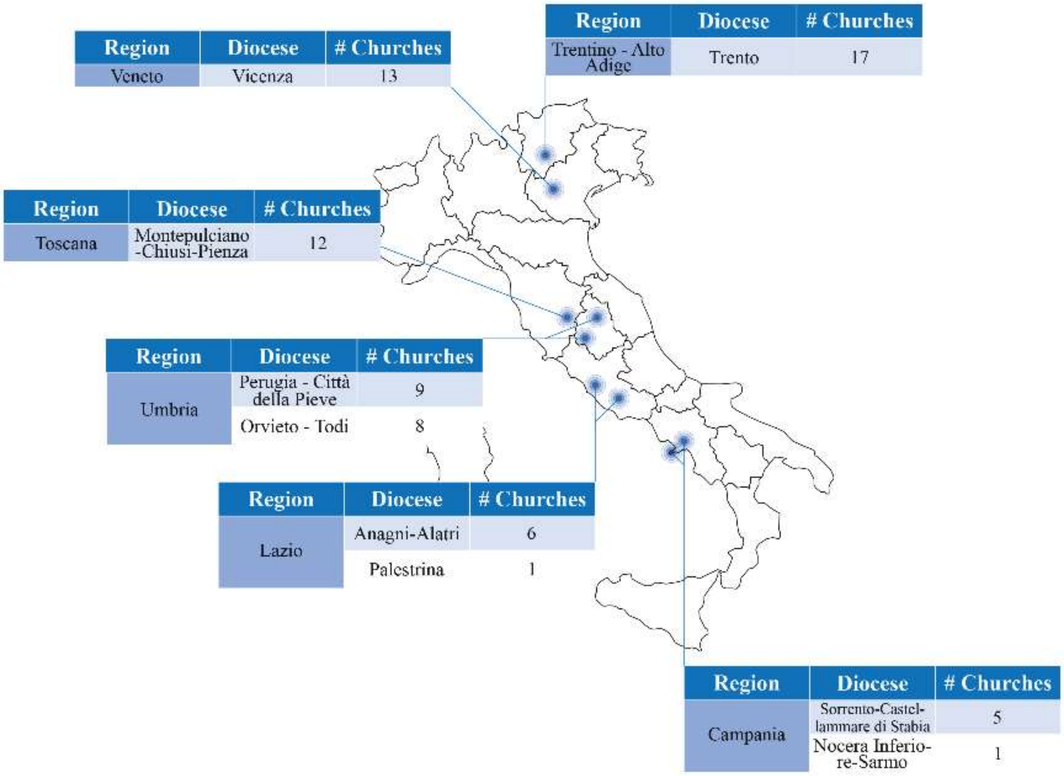

Figure 2 – Map of Italy indicating regional boundaries and the location of the nine dioceses in which churches were surveyed.

Within the current research, 72 churches in six different regions were surveyed (Figure 2). The complete list of the churches is tabulated in Pirchio 2020, Table A1. The surveyed churches were selected to be a representative sample of the stock of URM churches in each surveyed region based on four criteria, which are described in detail in Pirchio et al. [15]:

- The geographic location (considering the seismicity, the density of churches, the climate and geologic/topographic conditions, and the cultural and historic features);
- The churches' active functionality;
- The original construction period; and
- The urban and planimetric layout.

Due to the slenderness of church walls compared to most other types of buildings, churches and other complex URM buildings are best assessed for seismic vulnerability by subdividing them into structural sub-units vulnerable to damage and/or collapse called "macro-blocks" [6, 39, 40]. In general, in URM churches different macro-blocks types can be recognized (Figure 3). Most of the macro-block types – with the exception of the roof, which is usually in timber – are constructed in URM. In the current research, only the nine URM macro-block types were addressed, and, wherever visible (e.g., not covered in plaster), the URM type of each macro-block component was identified and assessed via NDT techniques.

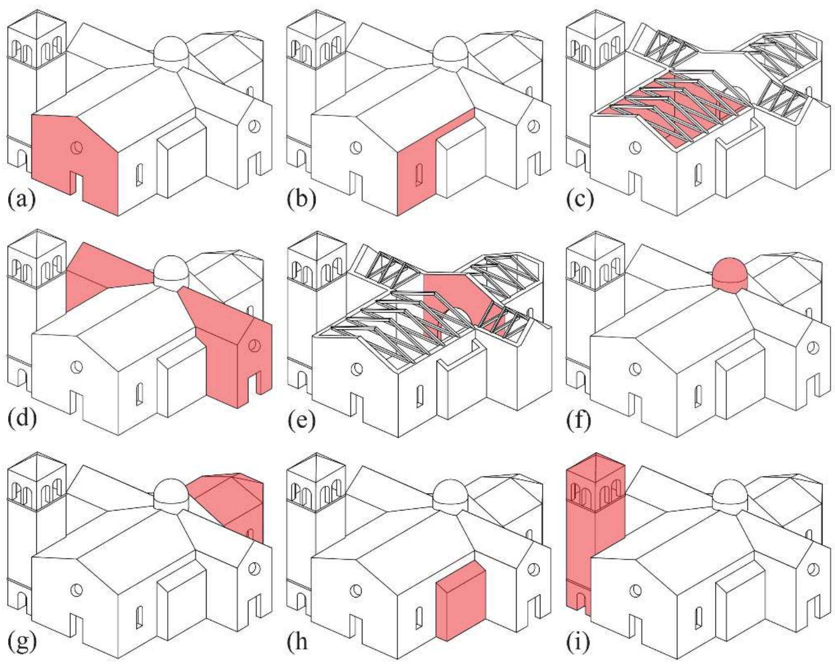

Figure 3 – Macro-blocks considered: (a) façade; (b) lateral walls; (c) naves; (d) transept; (e) triumphal arch; (f) dome; (g) apse; (h) chapels; (i) bell tower.

Four general URM types were found to be commonly used in the construction the macro-blocks components of the surveyed churches. The URM types were classified accordingly with MIT 2019 [32]:

- Irregular stone, with pebbles, erratic and irregular stone units (Figure 4a);
- Roughly cut stone with good bond (Figure 4b);
- Ashlar masonry with regular squared blocks and mortar joints (Figure 4c); and
- Solid fired clay bricks with lime mortar (Figure 4d).

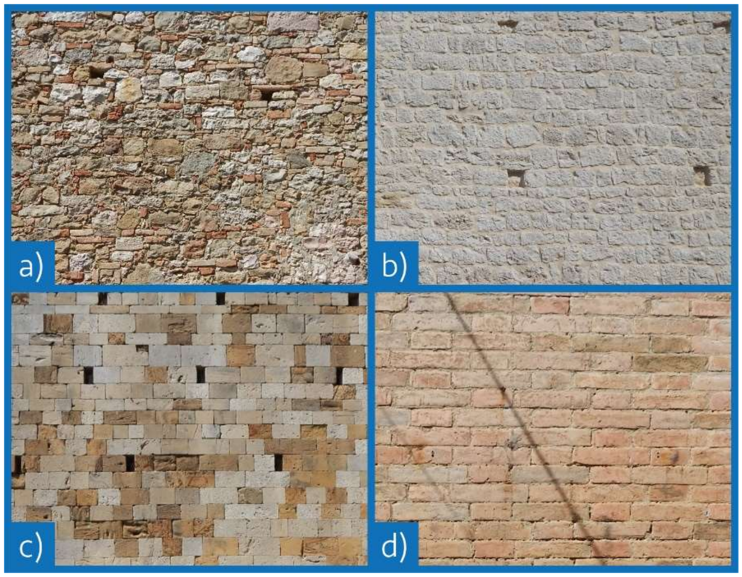

Figure 4 – Prototypical examples of URM types identified: a) irregular stone masonry, with pebbles, erratic and irregular stone units; b) roughly cut stone with good bond; c) ashlar masonry with regular squared blocks and mortar joints; d) solid fired clay bricks with lime mortar.

In total, 424 individual macro-blocks components were surveyed amongst the 72 churches (roughly six macro-blocks types for each church, in average). Given that some macro-blocks components were composed by different URM types due restorations over the time, 1.11 URM specimens were identified (in average) for each macro-block component resulting in 471 URM specimens. However, 268 masonry URM specimens (the 57%) were classified as "unknown" since the corresponding macro-blocks components resulted completely plastered. Although all the remaining 203 URM specimens were categorized accordingly with the four URM types (Figure 4), only the specimens in which all the NDT techniques could be applied (i.e., accessible) were considered in the current research, resulting in 170 tested URM specimens. In Table 1, the 170 tested URM specimens were categorized based on the recognized URM type.

URM type	Total tested specimens
Irregular stone, with pebbles, erratic and irregular stone units	20
Roughly cut stone with good bond	41
Ashlar masonry with regular squared blocks and mortar joints	75
Solid fired clay bricks with lime mortar	34

Table 1 – Total number of tested specimens and corresponding URM type.

78% of the surveyed churches were composed of at least five macro-block types, and the average church surveyed was identified as having six macro-blocks types. Given that roughly one URM specimen was tested for each macroblock and that the number of macro-blocks for each church was found to be relatively independent from the church's footprint dimensions, larger churches were not overly represented in the current research. In Figures 5 – 10, the distribution amongst the regions of the number of surveyed churches, the number of macro-blocks components identified for each one of the nine considered macro-blocks types, the number of different URM types identified in each macro-block component, and the total number of URM specimens for each one of the four URM type are illustrated.

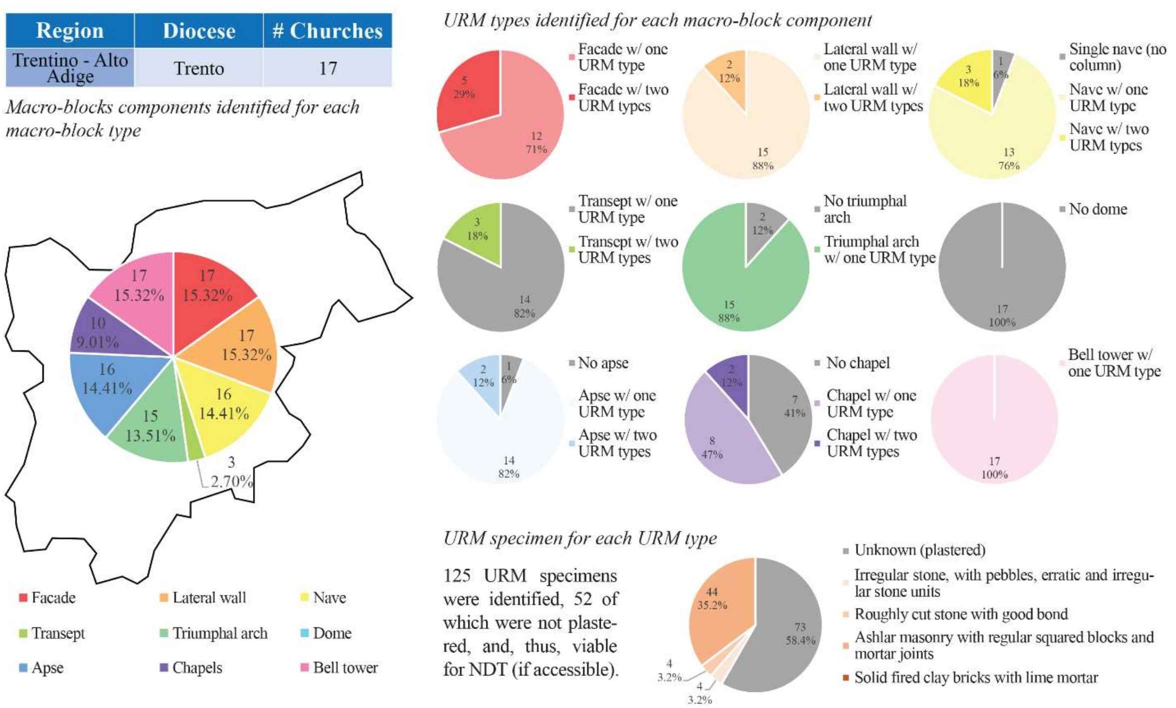

Figure 5 – Region: Trentino – Alto Adige; top left: number of surveyed churches; bottom left: number of macro-blocks components identified for each macro-block type; top right: number of URM types identified for each macro-block component; bottom right: number of URM specimen for each URM type.

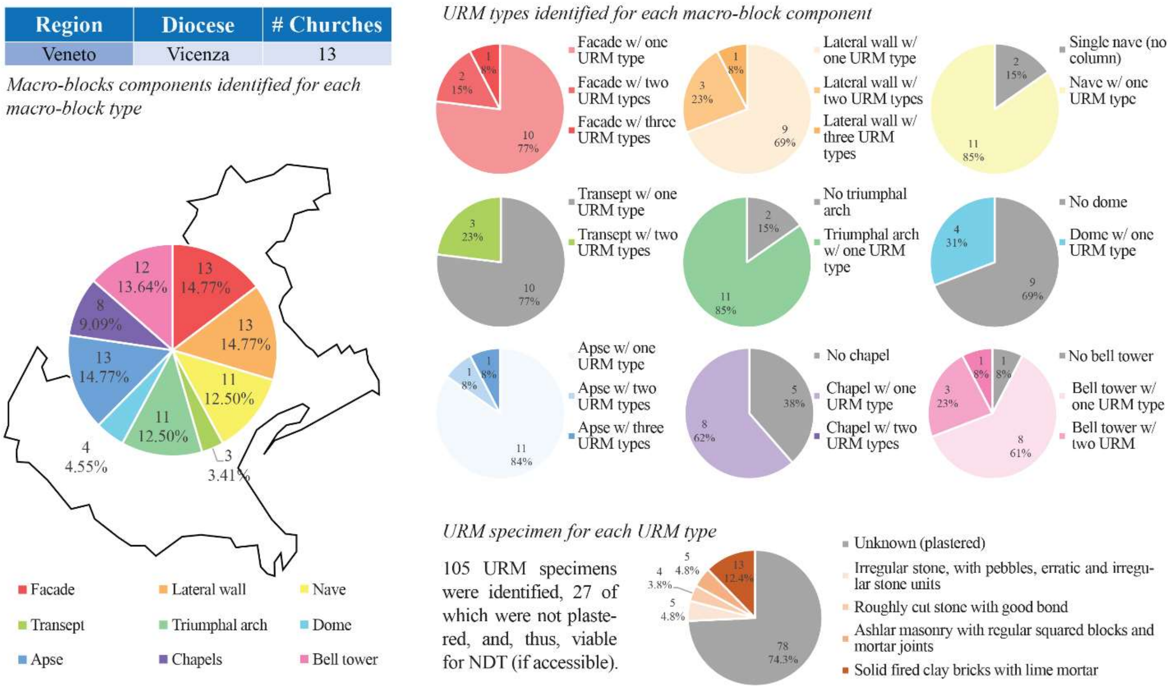

Figure 6 – Region: Veneto; top left: number of surveyed churches; bottom left: number of macro-blocks components identified for each macro-block type; top right: number of URM types identified for each macro-block component; bottom right: number of URM specimen for each URM type.

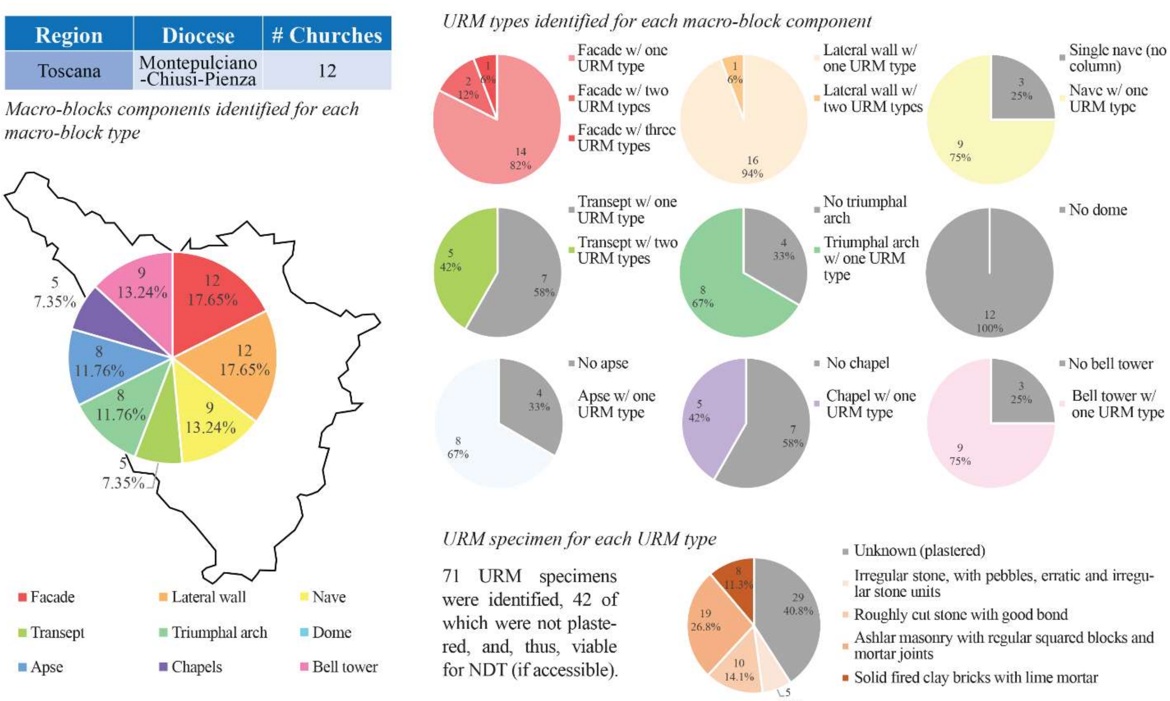

Figure 7 – Region: Toscana; top left: number of surveyed churches; bottom left: number of macro-blocks components identified for each macro-block type; top right: number of URM types identified for each macro-block component; bottom right: number of URM specimen for each URM type.

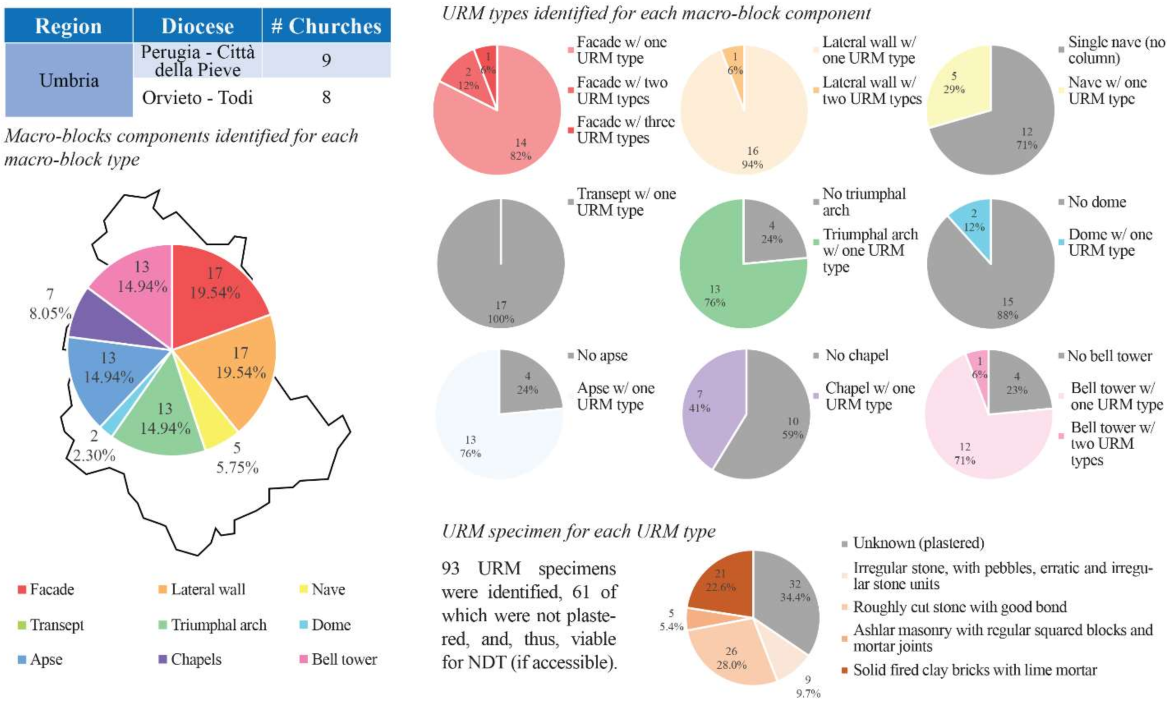

Figure 8 – Region: Umbria; top left: number of surveyed churches; bottom left: number of macro-blocks components identified for each macro-block type; top right: number of URM types identified for each macro-block component; bottom right: number of URM specimen for each URM type.

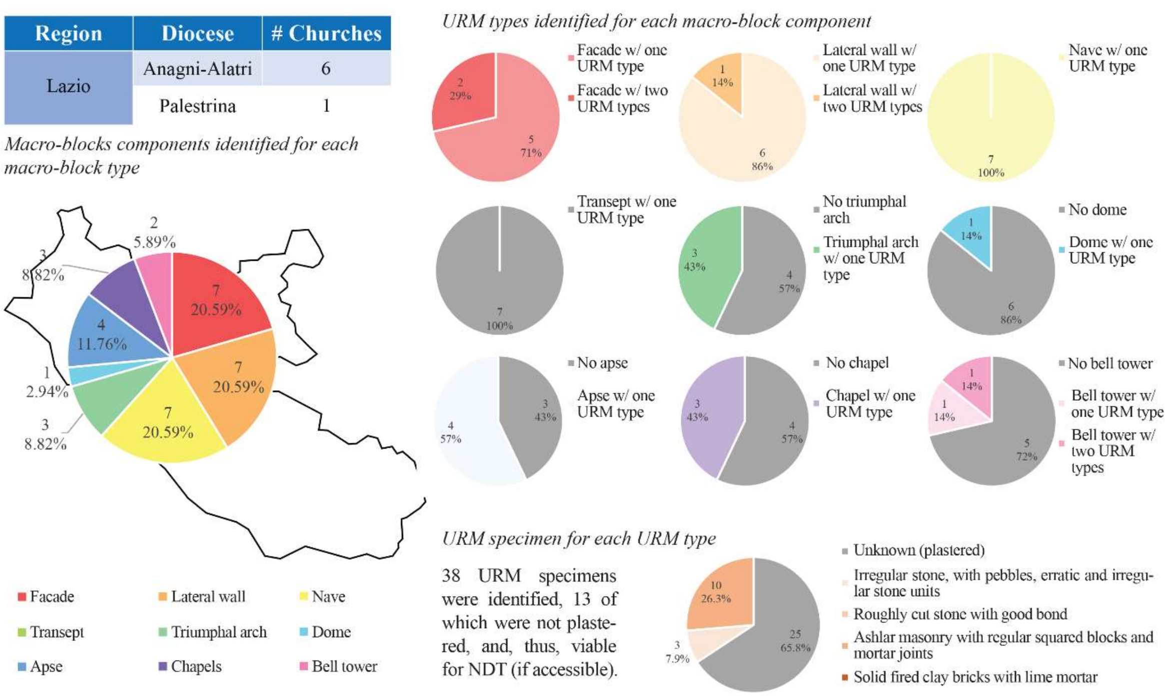

Figure 9 – Region: Lazio; top left: number of surveyed churches; bottom left: number of macro-blocks components identified for each macro-block type; top right: number of URM types identified for each macro-block component; bottom right: number of URM specimen for each URM type.

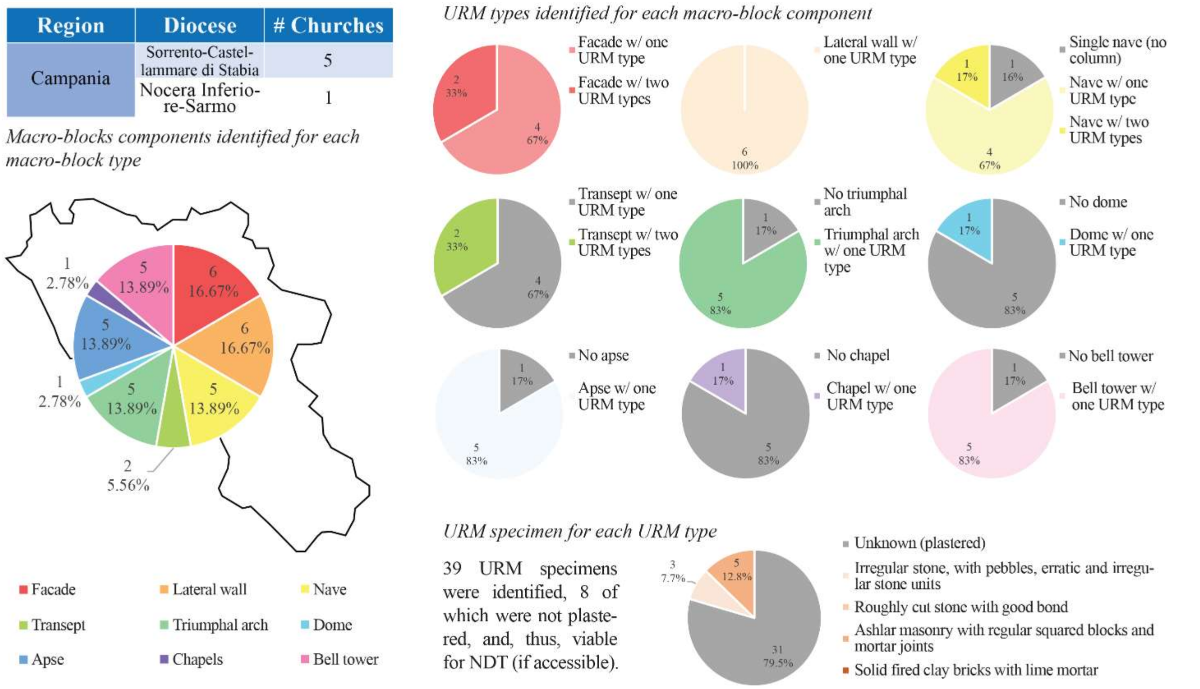

Figure 10 – Region: Campania; top left: number of surveyed churches; bottom left: number of macro-blocks components identified for each macro-block type; top right: number of URM types identified for each macro-block component; bottom right: number of URM specimen for each URM type.

Two NDT techniques were applied on the 170 tested URM specimens: 1) Schmidt hammer test; and 2) pulse velocity test. Furthermore, two expert judgment-based techniques were applied to define reasonable ranges of variation of the determined mechanical properties for each URM type: 1) the mechanical properties' range offered by MIT 2019 [32]; and 2) the masonry quality index (MQI). While both the NDT techniques and expert judgment-based techniques were described in further details in Section 3 of the current study, the criteria considered for their selection were listed in Table 2 relatively to each technique. Note that the terms "MIT 2019 ranges" and "MQI" used in Table 2 refer to the two aforementioned expert judgment-based techniques, respectively, the assessment of the mechanical properties ranges as defined by MIT 2019 [32], and via use of the masonry quality index [41, 34].

Criteria	Schmidt hammer test	Pulse velocity test	MIT 2019 ranges	MQI
Execution time	Very low	Low	n/a	Moderate
Test cost	Very low	Low	n/a	n/a
Independent of engineering judgment	Yes	Yes	No	No

Criteria	Schmidt hammer test	Pulse velocity test	MIT 2019 ranges	MQI
Equations based on large statistical base of destructive tests performed in the same country where the specimens were assessed (i.e, Italy)	No	No	Yes	Yes
Significant variation of the output for specimens "visually" homogeneous	Yes	Yes	No	No
Applicable when the masonry is not visible (i.e., plastered surface)	No	Yes (Although the plaster may affect the results)	No	No
Mechanical properties categorized by URM type	No	No	Yes	No
Multiple parameters are accounted for (with respect to both constitutive materials and construction technique)	No	No	No	Yes
Assumption of an a-priori probabilistic distribution of the mechanical properties	No	No	Yes	Yes

Table 2 – Selection criteria of the applied NDT and expert judgment techniques.

The two NDT techniques and the two expert judgment techniques have complementary benefits, as identified in Table 2 providing, therefore, a basis for the methodology proposed in the current research to assess the mechanical properties (i.e., masonry compressive strength, Young's modulus, and shear strength) of URM used to construct Italian medieval churches.

3. Non-destructive Testing (NDT) Techniques

3.1. Rebound Hammer Testing

The Schmidt hammer test is one of the most applied NDT techniques [42, 43, 44]. The test results in the measurement of the superficial hardness of the construction material (i.e., the bricks or the stones) based on the principle that the elastic energy absorbed by the material is correlated with its strength. However, the results may be affected by several factors (e.g., the roughness of the surface, the temperature, and the non-homogeneity of the material); thus, a strategic selection and preparation of the tested surface might be desirable.

In the current study, the tests were performed on any accessible and unplastered macro-block element in accordance with international standards [45, 46] . A Type L Schmidt hammer with a lens-shaped punch ending was used (Figure 11a), while the testing area (or areas if more than one URM type was identified in the same macro-block) was selected as the most visually representative of the entire macro-block surface. To increase the consistency of the testing results among different specimens, an 800 × 800 mm^2 grid with 200 mm spacing was applied to each tested surface (Figure 11b), and the test was performed on the unit at the center of each square of the grid resulting in 16 rebound numbers that were averaged to determine the mean rebound number of the specimen, *R*. In accordance with ASTM C805/C805M [45], readings differing more than six units from the mean rebound number were discarded. However, given the inherently variability of the units (i.e., brick or stones) when compared with concrete for which the standard was intended, the entire set of readings was not discarded in case of more than two readings differing more than six units from the mean. Nonetheless, the entire set of readings was discarded if less than ten rebound numbers resulted acceptable (i.e., differing more than six units from the mean rebound number). Mean analysis was applied on the valid readings of the set of readings to determine the mean rebound number, *R*.

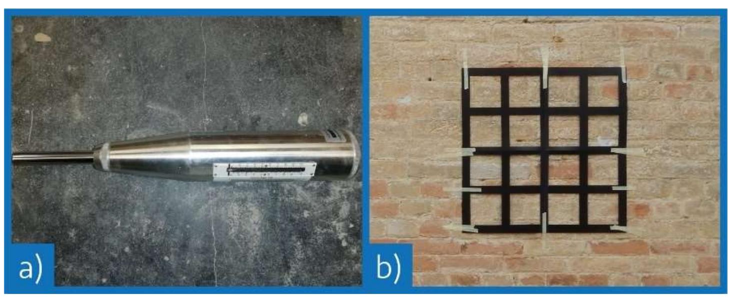

Figure 11 – a) type L Schmidt hammer; b) grid utilized for Schmidt hammer tests.

Given that the Schmidt hammer test can be only applied on the masonry units (i.e., the bricks or the stones), the application of these measurements for the identification of the masonry prism (i.e., unit and mortar) mechanical properties might seem inappropriate. In the current research, however, the mean rebound number, *R*, was aggregated with the pulse velocity test (discussed in the subsequent section) to establish a correlation to characterize the masonry prism as a whole accounting both for the properties of the bricks and the mortar as described in Section 5.

The mean rebound numbers for the 170 tested URM specimens are shown grouped by URM type and region in Figure 12. The values of *R* for each URM specimen are also listed in Table B1 through B4 in Appendix B grouped by URM type.

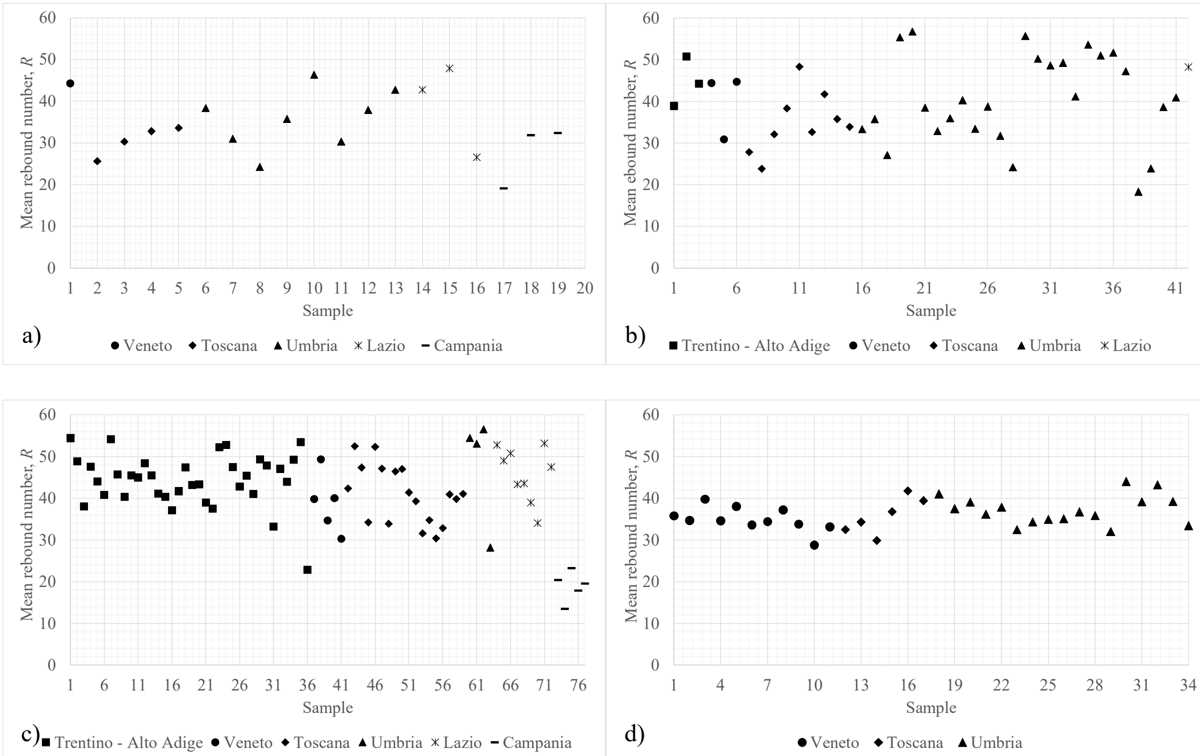

Figure 12 – Mean rebound numbers grouped by URM type and region: a) irregular stone, with pebbles, erratic and irregular stone units; b) roughly cut stone with good bond; c) ashlar masonry with regular squared blocks and mortar joints; d) solid fired clay bricks with lime mortar.

3.2. Pulse Velocity Test

The pulse velocity test is an NDT technique used to measure the velocity of the ultrasonic waves passing through a masonry wall. The ultrasonic pulse is emitted by and received by two transducers (Figure 13a) while the mean velocity of the pulse is determined dividing the distance between the centers of the transducers by the time interval between the signal emission from the first transducer and the signal reception by the second transducer. While the pulse velocity test might be applied to evaluate the uniformity of the masonry, to estimate the depth of cracks, and to detect the presence of internal voids [21, 47, 48], in the current research it was applied to estimate the compressive strength of the masonry, f'_m, and the Young's modulus, E_m.

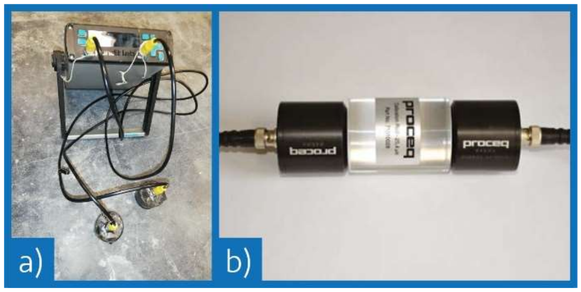

Figure 13 – a) Ultrasonic pulse velocity tester; b) Calibration control sample.

The pulse velocity tests were performed on any accessible macro-block element in accordance with international standards [49, 50, 51]. The ultrasonic pulse velocity tests were conducted in the same wall area in which the Schmidt hammer test was performed for each element. Plasticine medallions were applied on the transducer surface after proving that the resulting pulse velocity would be unaffected based on a calibration sample (Figure 13b). Although ASTM C597 [49] describes the direct and the semi-direct configurations of the test (Figure 14a and b) as the most accurate, and specify to perform the test accordingly whenever possible, in most cases reaching simultaneously two faces of the tested macro-block elements was unfeasible because of the thickness of the wall, the lack of openings, or other various obstacles. Hence, to achieve more consistency among the measurements for different macro-blocks, all tests in the current research were conducted using the indirect configuration (Figure 14c) with a pulse frequency of 54 kHz to allow a deeper penetration of the sonic wave into the masonry.

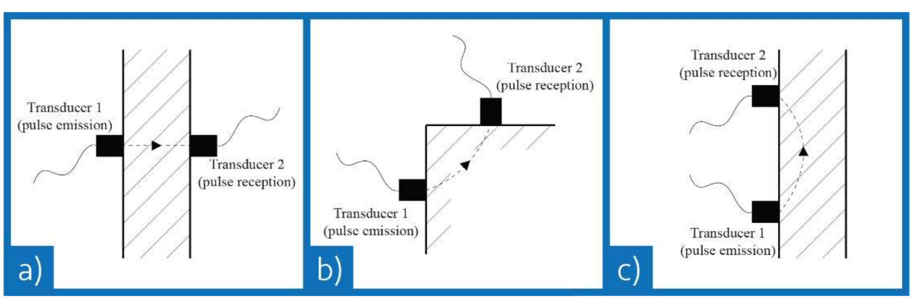

Figure 14 – Pulse velocity test configuration: a) direct; b) semi-direct; c) indirect.

The distance between the centers of the transducers was varied specimen-by-specimen based on the different URM types (i.e., brickwork or stonework) to ensure that the pulse velocity waves passed through both the masonry units and the mortar beds, ranging between 150 mm and 400 mm. At least three readings were taken for each specimen, and the specimen pulse velocity, v_i, was taken as the mean of the measurements. In cases in which the readings were differing more than 30% from the mean pulse velocity and, hence, internal damage or crack in the URM (either the units or the mortar) was suspected, three additional readings at nearby locations were taken. However, none of the readings was excluded from the mean as damage in the URM may affect the mechanical properties and the possibility of internal cracks at other locations of the macro-block could not be ignored.

The mean indirect pulse velocities, v_i, for the 170 tested URM specimens are shown grouped by URM type and region in Figure 15. The values of v_i for each URM specimen are also listed in Table B1 through B4 in Appendix B grouped by URM type. Considering that the Young's modulus of a generic material is proportional to the square of the pulse velocity [52], it was expected that the largest mean velocities were found to correspond to the ashlar masonry with regular squared blocks and mortar joints (Figure 15c) as this URM type has a larger unit-to-mortar ratio, and therefore, larger Young's modulus. The most consistent readings, instead, were found to correspond to the URM made of solid fired clay bricks with lime mortar (Figure 15d). The latter finding might be explained by the fact that ashlar is frequently limited to the external leaf while the internal one and the inner core are frequently much less regular and presenting a larger amount of mortar.

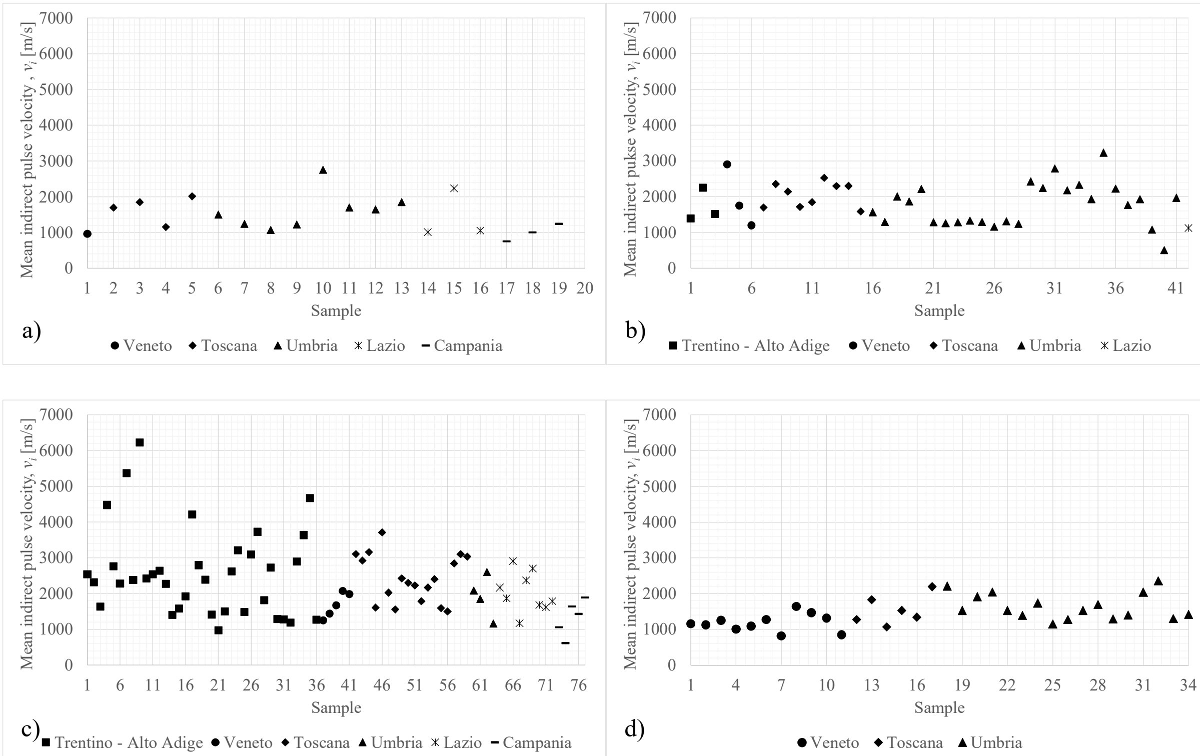

Figure 15 – Mean indirect pulse velocity grouped by URM type and region: a) irregular stone, with pebbles, erratic and irregular stone units; b) roughly cut stone with good bond; c) ashlar masonry with regular squared blocks and mortar joints; d) solid fired clay bricks with lime mortar.

4. Expert Judgment Techniques

4.1. URM Type Mechanical Property Ranges based on MIT 2019

MIT 2019 [32] provides a qualitative method to determine ranges for the assessment of the mechanical properties of existing URM and corrective coefficients to apply for different scenarios.

The URM type mechanical property ranges and the maximum corrective coefficients proposed by MIT 2019 [32] for the assessment of different existing URM types are listed in Table 3 and Table 4.

URM type	f'_m [MPa]	c [MPa]	E_m [MPa]	G_m [MPa]	w [kN/m^3]
	min – max	min – max	min – max	min – max	
Rubble stones	1.0 – 2.0	0.018 – 0.032	690 – 1050	230 – 350	19
Hewn ashlar, with non-homogenous leaves	2.0	0.035 – 0.051	1020 – 1440	340 – 480	20
Split stones with good texture	2.6 – 3.8	0.056 – 0.074	1500 – 1980	500 – 660	21
Irregular masonry with soft stone blocks (tuff, calcarenite, etc.)	1.4 – 2.2	0.028 – 0.042	900 – 1260	300 – 420	13 – 16
Regular masonry with soft stone blocks (tuff, calcarenite, etc.)	2.0 – 3.2	0.04 – 0.08	1200 – 1620	400 – 500	
Squared stone blocks	5.8 – 8.2	0.09 – 0.12	2400 – 3300	800 – 1100	22
Solid fired clay bricks with lime mortar	2.6 – 4.3	0.05 – 0.13	1200 – 1800	400 – 600	18

URM type	f'_m [MPa]	c [MPa]	E_m [MPa]	G_m [MPa]	w [kN/m^3]
	min – max	min – max	min – max	min – max	
Semi-solid fired clay bricks with cement mortar	5.0 – 8.0	0.08 – 0.17	3500 – 5600	875 – 1400	15

Table 3 – Mechanical properties of different URM types. Values adopted by the MIT 2019 [32].

URM type	As-built condition			Strengthening intervention			
	Good-quality mortar (c_1)	Presence of horizontal courses (c_2)	Leaves connectors (c_3)	Mortar grouting (c_4)	Reinforced Plaster (c_5)	Reinforced repointing and leaves connectors (c_6)	Maximum coefficient (c_{max})
Rubble stones	1.5	1.3	1.5	2.0	2.5	1.6	3.5
Hewn ashlar, with non-homogenous leaves	1.4	1.2	1.5	1.7	2.0	1.5	3.0
Split stones with good texture	1.3	1.1	1.3	1.5	1.5	1.4	2.4
Irregular masonry with soft stone blocks (tuff, calcarenite, etc.)	1.5	1.2	1.3	1.4	1.7	1.1	2.0
Regular masonry with soft stone blocks (tuff, calcarenite, etc.)	1.6	-	1.2	1.2	1.5	1.2	1.8
Squared stone blocks	1.2	-	1.2	1.2	1.2	-	1.4
Solid fired clay bricks with lime mortar	-	-	1.3	1.2	1.5	1.2	1.8
Semi-solid fired clay bricks with cement mortar	1.2	-	-	-	1.3	-	1.3

Table 4 – Maximum corrective coefficients for different URM types. Values adopted by MIT 2019 [32].

According to MIT 2019 [32], the coefficients listed in Table 4 should be applied consistently with the following criteria:

- The coefficient c_1 can be applied both to the strengths (f'_m and c) and to the elastic moduli (E_m and G_m);
- The coefficient c_2 can be applied only to the strengths (f'_m and c);
- The coefficient c_3 can be applied only to the strengths (f'_m and c);
- The coefficient c_4 can be applied both to the strengths (f'_m and c) and to the elastic moduli (E_m and G_m), but the benefit might be neglected if the original mortar has a good quality;

- The coefficient c_5 can be applied both to the strengths (f'_m and c) and to the elastic moduli (E_m and G_m), but the benefit might be neglected if the wall has systematic leaves connectors;
- The coefficient c_6 can be fully applied to the strengths (f'_m and c) and with a 50% reduction to the elastic moduli (E_m and G_m), but the benefit might be neglected if reinforced plaster is applied to the wall;
- More than one coefficient might be applied to the same URM type without exceeding the maximum incremental coefficient c_{max}; and
- In case of poor quality mortar, a reduction coefficient of 0.7 and 0.8 can be applied to the strength (f'_m and c) and the moduli (E_m and G_m), respectively.

By applying the corrective coefficients given in Table 4 to the base values for the URM types relevant for the current study, the strengths and moduli ranges listed in Table 5 were obtained. It might be noticed that in the ranges identified by MIT 2019 [32] (Table 5) the variation in strength and moduli within the same URM type is significant, with maximum values that could be ten times larger than the minimum ones. Therefore, small variations in the application of the corrective coefficients given in Table 4 (i.e., different evaluations based on the expert judgment of the surveyor) may result in major changes in the assumptions for the URM mechanical properties.

URM type	f'_m [MPa]	E_m [MPa]	G_m [MPa]	w [kN/m³]
	min – max	min – max	min – max	
Irregular stone, with pebbles, erratic and irregular stone units	0.70 – 7.00	552 – 3675	184 – 1225	19
Roughly cut stone with good bond	1.82 – 9.12	1200 – 3861	400 – 1287	20
Ashlar masonry with regular squared blocks and mortar joints	4.06 – 11.48	1920 – 4620	640 – 1540	21
Solid fired clay bricks with lime mortar	1.82 – 7.74	960 – 2700	320 – 900	18

Table 5 – Ranges of the mechanical properties for the considered URM types according to MIT 2019 [32].

4.2. Masonry Quality Index (MQI)

The masonry quality index (*MQI*) is an expert-judgement score-based method developed by Borri et al. [41] to classify the behavior of URM under three possible scenarios: 1) vertical loading (*V*); 2) horizontal in-plane loading (*I*); and 3) horizontal out-of-plane loading (*O*), and to estimate upper and lower bounds for related mechanical parameters. The *MQI* accounts for seven different parameters related to the composing materials of the URM (i.e., units and mortar) and constructive characteristics of the URM. Each parameter is defined by three possible categories with respect to the established rule of art: 1) fulfilled, *F*; 2) partially fulfilled, *PF*; and 3) not fulfilled, *NF*. The seven assessed parameters were defined as follows by Borri, et al. [41]:

- The state of conservation and the mechanical properties (*SM*) of the masonry units (bricks or stones);
- The stone/brick dimension properties (*SD*);
- The stone/brick shape (*SS*);
- The wall leaves connection (*WC*);
- The horizontal joints characteristics (*HJ*);
- The vertical joints characteristics (*VJ*); and
- The mortar mechanical properties (*MM*).

The *MQI* was determined for each loading direction by converting the categories of the assessment (i.e., *NF*, *PF*, and *F*) into quantitative values according to the criteria listed in Table 6. The original Equation for computing *MQI* [41] has been recently updated by Borri and De Maria [33] and can be generalized as follows:

$$MQI_{V\ or\ I} = m \cdot r \cdot g \cdot SM \cdot (SD + SS + WC + HJ + VJ + MM) \qquad (1)$$

where: MQI_V and MQI_I are the value of the masonry quality index with respect to the vertical loading and horizontal in-plane loading, respectively; and

m and r are coefficients related to mortar characteristics and g is a coefficient related to bed joint thickness, as listed in Table 7.

The criteria used to convert the categorical outcomes of the assessment (i.e., *NF*, *PF*, and *F*) into numerical values to be applied in Equation 1 to determine the *MQI* [33] are listed in Table 6 and Table 7.

Parameter	Vertical loading (*V*)			Horizontal in-plane loading (*I*)			Horizontal out-of-plane loading (*O*)		
	NF	***PF***	***F***	***NF***	***PF***	***F***	***NF***	***PF***	***F***
SM	0.3	0.7	1.0	0.3	0.7	1.0	0.5	0.7	1.0
SD	0	0.5	1.0	0	0.5	1.0	0	0.5	1.0
SS	0	1.5	3.0	0	1.0	2.0	0	1.0	2.0
WC	0	1.0	1.0	0	1.0	2.0	0	1.5	3.0
HJ	0	1.0	2.0	0	0.5	1.0	0	1.0	2.0
VJ	0	0.5	1.0	0	1.0	2.0	0	0.5	1.0
MM	0	0.5	2.0	0	1.0	2.0	0	0.5	1.0

Table 6 – Numerical values for determining the MQI. Values adopted from Borri et al. [41].

Parameter	Vertical loading (*V*)	Horizontal in-plane loading (*I*)	Horizontal out-of-plane loading (*O*)
m	0.7 for bad quality mortar	0.7 for bad quality mortar	0.7 for bad quality mortar
	1.0 in all the other cases	1.0 in all the other cases	1.0 in all the other cases
g	0.7 for solid fired clay bricks with mortar joints thicker than 13mm	0.7 for solid fired clay bricks with mortar joints thicker than 13mm	0.7 for solid fired clay bricks with mortar joints thicker than 13mm
	1.0 in all the other cases	1.0 in all the other cases	1.0 in all the other cases
r	0.2 if *MM* = *NF*	1.0 if *MM* = *NF*	0.1 if *MM* = *NF*
	0.6 if *MM* = *PF*	1.0 if *MM* = *PF*	0.85 if *MM* = *PF*
	1.0 if *MM* = *F*	1.0 if *MM* = *F*	1.0 if *MM* = *F*

Table 7 – Numerical values for the parameters m, g, *and* r.

Loading direction	URM category		
	A	***B***	***C***
Vertical loading (*V*)	$10 \geq MQI_V > 5$	$5 \geq MQI_V > 2.5$	$2.5 \geq MQI_V \geq 0$
In-plane loading (*I*)	$10 \geq MQI_I > 5$	$5 \geq MQI_I > 3$	$3 \geq MQI_I \geq 0$
Out-of-plane loading (*O*)	$10 \geq MQI_O > 7$	$7 \geq MQI_O > 4$	$4 \geq MQI_O \geq 0$

Table 8 – Masonry categories as a function of the MQI. Values adopted from Borri et al. [41].

The *MQI* may be also used for a categorical classification of the macroblock behavior with respect to the direction of loading (Table 8), which might have applications in conventional risk assessment [15]. Basing on the response to the different loading direction, three URM categories were identified: 1) good response, *A*; 2) response of average quality, *B*; and 3) inadequate response, *C*.

Additionally, Borri and De Maria [33] also proposed correlations of the relevant *MQI* with upper and lower bounds of the mechanical properties of the masonry (i.e., the masonry compressive strength (f'_m), and the elastic moduli (E_m, G_m). The correlations are shown in Equation 2 – 4 [33].

$$1.036e^{0.1961MQI_V} \leq f'_m = 1.4211e^{0.1844MQI_V} \leq 1.8021e^{0.1775MQI_V} \quad (2)$$

$$599.03e^{0.1567MQI_V} \leq E_m = 731.51e^{.1548MQI_V} \leq 863.74e^{0.1535MQI_V} \quad (3)$$

$$204.50e^{0.1464MQI_I} \leq G_m = 247.62e^{0.1457MQI_I} \leq 290.56e^{0.1452MQI_I} \quad (4)$$

In Figure 16, the MQI_V for vertical loading of the 170 URM specimens in the current research are shown grouped by URM type and region. The values of the *MQI* for vertical and horizontal in-plane loading (MQI_V and MQI_I respectively) of each URM specimen are also listed in Table B1 through B4 in Appendix B grouped by URM type. The values of the *MQI* for out-of-plane loading (MQI_O) were not reported in the current research since it was not used in any calculation. It might be notice that the result for the *MQI* value presented large variability even within the same URM type and geographical region (Figure 16), however, URM made of irregular stone, with pebbles, erratic and irregular stone units (Figure 16a) was found to have, overall, lower *MQI* values mostly because of the irregular shapes of the units (*SS*) and of the mortar joints (*HJ* and *VJ*). URM made of ashlar masonry with regular squared blocks and mortar joints (Figure 16c), instead, generally corresponded to larger *MQI* values due to the large compressive strength of the units (*SM*), their dimensions (*SD*), and their shapes (*SS*). Finally, URM made of roughly cut stone with good bond and solid fired clay bricks with lime mortar (Figure 16b and c, respectively), resulted in highly variable *MQI* values, largely depending on the wall leaves connections (*WC*) and the vertical joints characteristics (*VJ*).

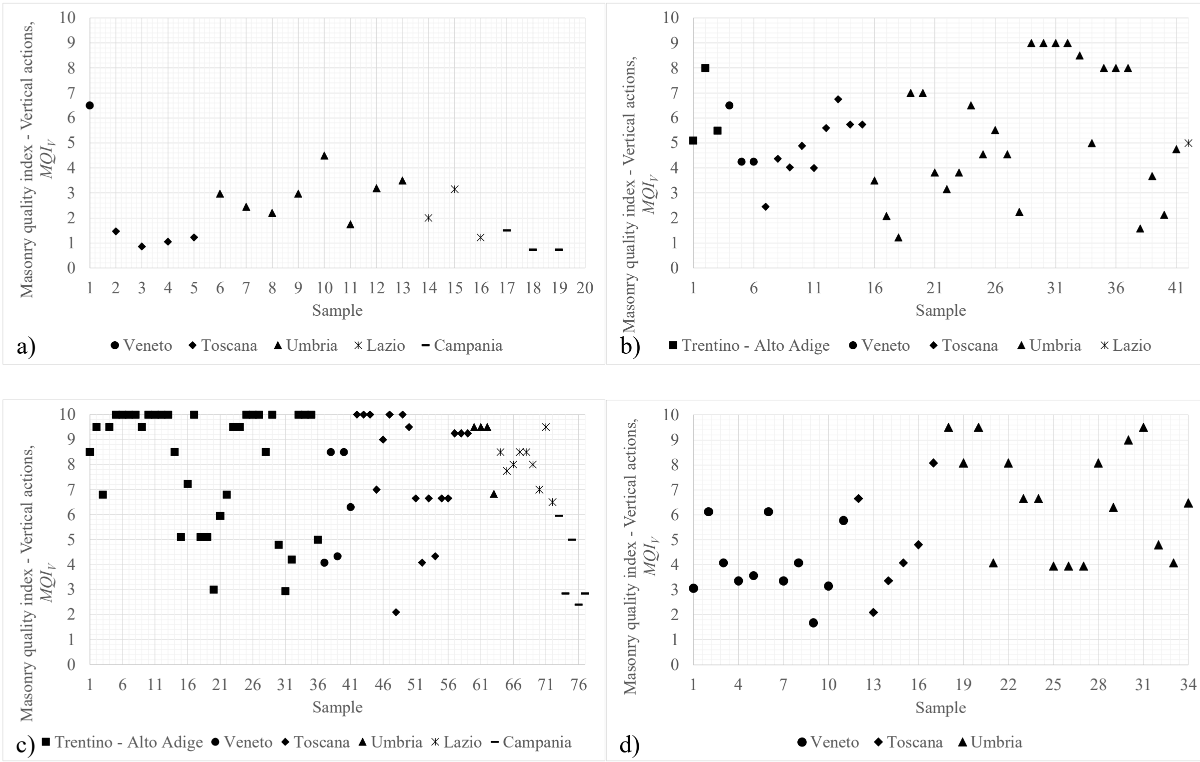

Figure 16 – MQI_V grouped by URM type and region: a) irregular stone, with pebbles, erratic and irregular stone units; b) roughly cut stone with good bond; c) ashlar masonry with regular squared blocks and mortar joints; d) solid fired clay bricks with lime mortar.

5. Aggregation of the two NDT techniques and the two expert judgment techniques

In the following sections the mechanical parameters estimated according to Equation 2 – 4, based on masonry quality index, will be correlated with rebound hammer number and pulse velocity, in terms of minimum of least square error. Consequently, it will be possible to estimate masonry compressive and shear strengths, as well as Young's and shear moduli, based on NDT techniques. Moreover, rebound hammer limits the uncertainties in the selection of the proper category of element state of conservation and mechanical properties, while pulse velocity test limits those about leaves connection, encouraging the use of NDT techniques over a procedure based only on expert judgement.

5.1. Masonry Compressive Strength, f'_m

According to several authors [35, 36, 37], the results of the Schmidt hammer test and the pulse velocity test can be combined into the SonReb method, a combined NDT technique which increases the reliability of the two tests when considered separately [42, 53]. The rebound number and the pulse velocity were combined using Equation 5. Although the SonReb method is usually applied to concrete specimens, the current research focused on applying the same procedure to URM specimens. Although different authors proposed values for the correlation coefficients for the SonReb approach as applied to concrete [35, 36, 37], and to stones/bricks [54, 55], the authors of the current research are not aware of reliable values to be applied to URM. Thus, given the impossibility of extracting samples from the URM macro-block tested in-situ, the more accredited *MQI* [33] method was used to calibrate the required correlation coefficients, a, b, and c for the SonReb approach. Therefore, the correlation coefficients, a, b, and c were regressed by best-fitting Equation 5 versus the mean compressive strength as determined using Equation 2.

$$f'_m = a{v_i}^b R^c \tag{5}$$

where: f'_m is the compressive strength of the masonry in MPa;

v_i is the pulse indirect velocity measured through the pulse velocity test in m/s;

R is the rebound number measured through the Schmidt hammer test;

a, b, and c are correlation coefficients to best-fit the equation.

The coefficients to apply in Equation 5 were determined for each URM type resulting in the values listed in Table 9.

URM type	Correlation coefficients		
	a	b	c
Irregular stone, with pebbles, erratic and irregular stone units	7.566×10^{-2}	1.000×10^{-2}	9.396×10^{-1}
Roughly cut stone with good bond	2.007×10^{-3}	5.497×10^{-1}	9.491×10^{-1}
Ashlar masonry with regular squared blocks and mortar joints	2.213×10^{-2}	3.602×10^{-1}	7.738×10^{-1}
Solid fired clay bricks with lime mortar	1.171×10^{-3}	5.796×10^{-1}	1.105

Table 9 – Correlation coefficients a, b, and c for each URM type.

In Figure 17, the compressive strength, f'_m, of the 170 URM specimens obtained by using Equation 5. The predicted values were hence compared with the lower and upper bounds given by the MQI method per Equation 2 (solid lines in Figure 17) and by mechanical property ranges per MIT

2019 [32] as shown in Table 5 (dashed lines in Figure 17). The standard errors of the regression, *S*, for each URM type are shown in Figure 17. It might be noticed that 98% of the predicted values of the compressive strength were encompassed by the identified lower and upper bounds (either per the MQI method or per the mechanical property ranges per MIT 2019 [32]).

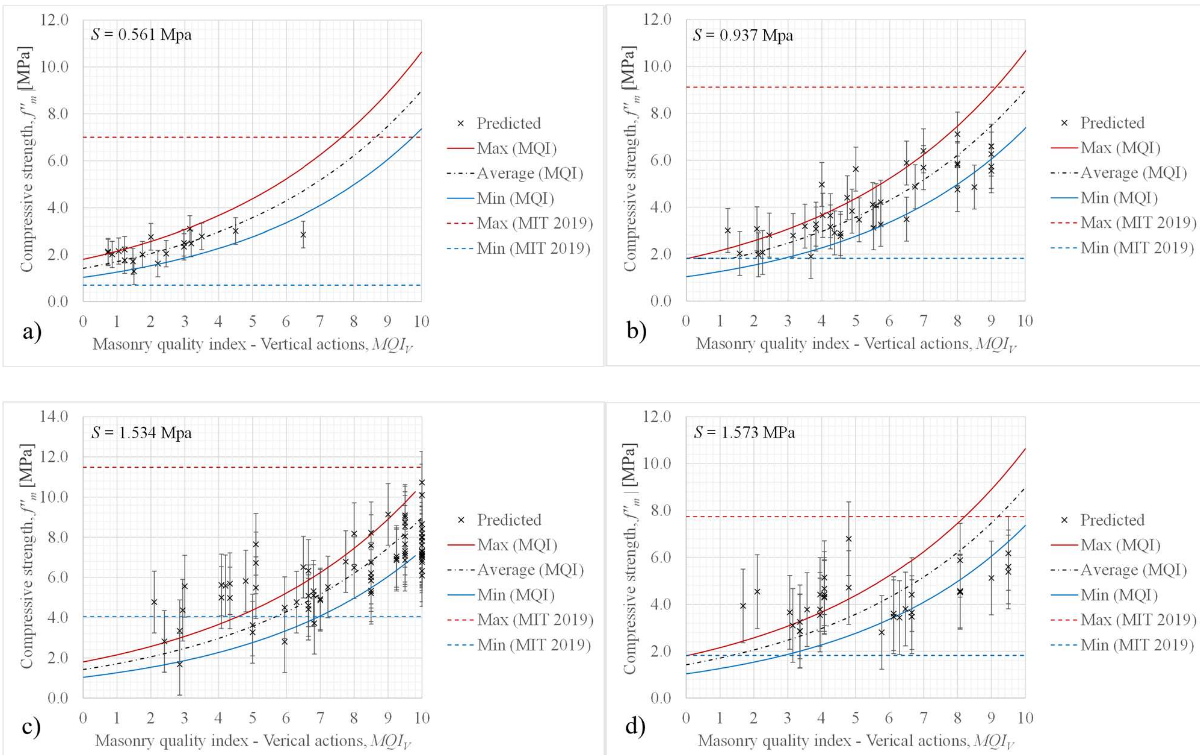

Figure 17 – The compressive strength f'_m of the URM specimens, estimated according to Eq. (7), grouped by URM type and compared with masonry quality index for vertical loading, MQI_V. a) irregular stone, with pebbles, erratic and irregular stone units; b) roughly cut stone with good bond; c) ashlar masonry with regular squared blocks and mortar joints; d) solid fired clay bricks with lime mortar.

5.2. Masonry Young's Modulus, E_m

Accordingly to different international standards [56, 57] and authors [58, 59], the Young's modulus of the masonry, E_m, can be determined proportionally to the compressive strength, f'_m, as shown in Equation 6.

$$E_m = K_{em} f'_m \tag{6}$$

where: E_m is the static elastic modulus (i.e., Young's modulus) of the masonry in MPa;

K_{em} is the proportion coefficient for the elastic modulus.

Similarly to what was done in Section 5.1 of the research, the proportion coefficient, K_{em}, was regressed by best-fitting Equation 6 versus the mean Young's modulus as determined using Equation 3. The values of K_{em} to apply in Equation 6 were determined for each URM type resulting in the values listed in Table 10.

URM type	Elastic modulus proportion coefficient, K_{em}
Irregular stone, with pebbles, erratic and irregular stone units	472
Roughly cut stone with good bond	423
Ashlar masonry with regular squared blocks and mortar joints	396
Solid fired clay bricks with lime mortar	423

Table 10 – Elastic modulus proportion coefficient, K_{em}, for each URM type.

In Figure 18, the Young's modulus, E_m, based on Equation 6 of the 170 URM specimens are shown grouped by URM type and compared with masonry quality index for vertical loading, MQI_V. The predicted values were hence compared with the lower and upper bounds given by the *MQI* method per Equation 3 (solid lines in Figure 18) and by mechanical property ranges per MIT 2019 [32] as shown in Table 5 (dashed lines in Figure 18). The standard errors of the regression, *S*, for each URM type are shown in Figure 18. It might be noticed that 96% of the predicted values of the Young's modulus were encompassed by the identified lower and upper bounds (either per the MQI method or per the mechanical property ranges per MIT 2019 [32]).

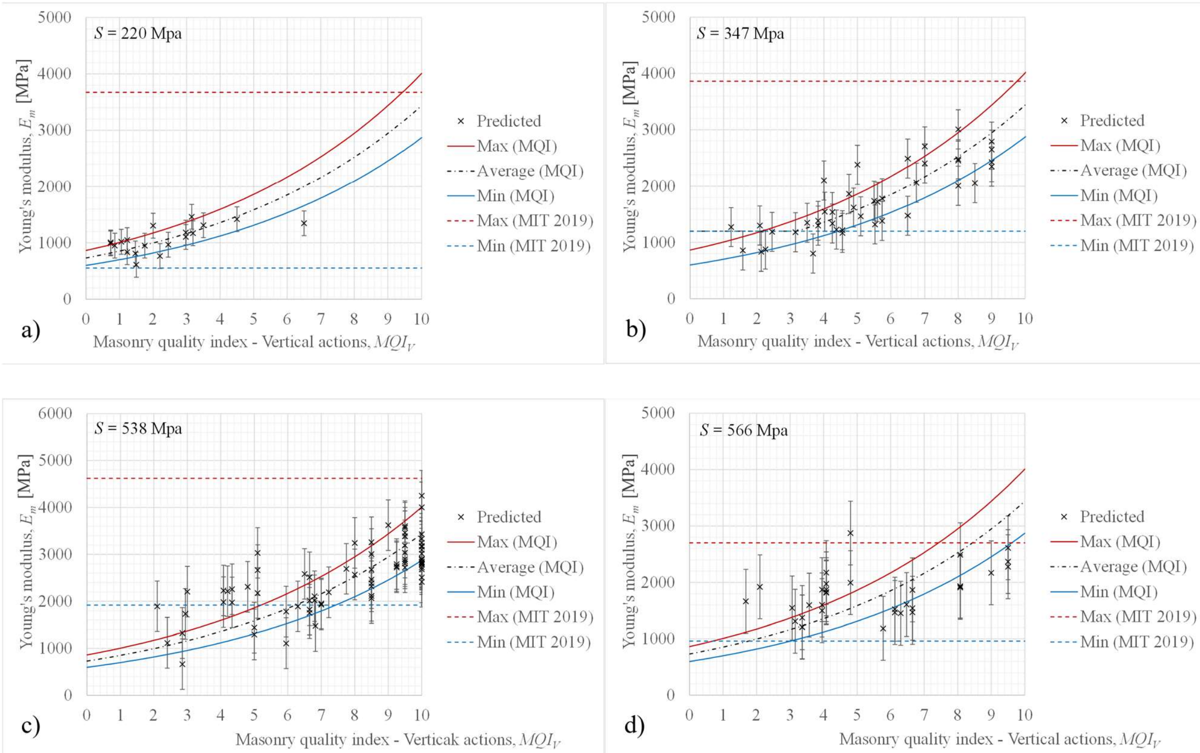

Figure 18 – The Young's modulus, E_m, based on Equation 10 of the URM specimens grouped by URM type and compared with masonry quality index for vertical loading, MQI_V. a) irregular stone, with pebbles, erratic and irregular stone units; b) roughly cut stone with good bond; c) ashlar masonry with regular squared blocks and mortar joints; d) solid fired clay bricks with lime mortar.

The determined proportion coefficients for the Young's modulus, K_{em}, are in accordance with the values proposed by other sources, as shown in Table 11.

URM type	Proposed proportion coefficient for the Young's modulus, K_{em}	K_{em} [56]	K_{em} [57]	K_{em} [58]	K_{em} [59]
Irregular stone, with pebbles, erratic and irregular stone units	472	550	300	210 - 1670	250 - 1100
Roughly cut stone with good bond	423				
Ashlar masonry with regular squared blocks and mortar joints	396				
Solid fired clay bricks with lime mortar	423				

Table 11 – Proposed elastic modulus proportion coefficient, K_{em}, compared with other authors.

5.3. Masonry Shear Modulus, G_m

According to the Eurocode [60] and to Bosiljkov, Totoev and Nichols [61] the shear modulus for URM, G_m, can be determined as proportional to the Young's modulus, E_m, as shown in Equation 7.

$$G_m = K_{es} E_m \quad (7)$$

where:

K_{es} is the proportion coefficient for the shear modulus.

Similarly to what was done in Section 5.1 of the research, the proportion coefficient for the shear modulus, K_{es}, was regressed by best-fitting Equation 7 versus the mean shear modulus as determined using Equation 4. The values of K_{es} to apply in Equation 7 were determined for each URM type resulting in the values listed in Table 12.

URM type	Proportion coefficient for the shear modulus, K_{es}
Irregular stone, with pebbles, erratic and irregular stone units	0.332
Roughly cut stone with good bond	0.312
Ashlar masonry with regular squared blocks and mortar joints	0.299
Solid fired clay bricks with lime mortar	0.348

Table 12 – Shear modulus proportion coefficient, K_{es}, for each URM type.

In Figure 19, the shear modulus, G_m, of the 170 URM specimens obtained by using the described technique are shown grouped by URM type and compared with masonry quality index for horizontal in-plane loading, MQI_I. The predicted values were hence compared with the lower and upper bounds given by the *MQI* method per Equation 4 (solid lines in Figure 19) and by mechanical property ranges per MIT 2019 [32] as shown in Table 5 (dashed lines in Figure 19). The standard errors of the regression, *S*, for each URM type are shown in Figure 19. It might be noticed that 94% of the predicted values of the Young's modulus were encompassed by the identified lower and upper bounds (either per the MQI method or per the mechanical property ranges per MIT 2019 [32]).

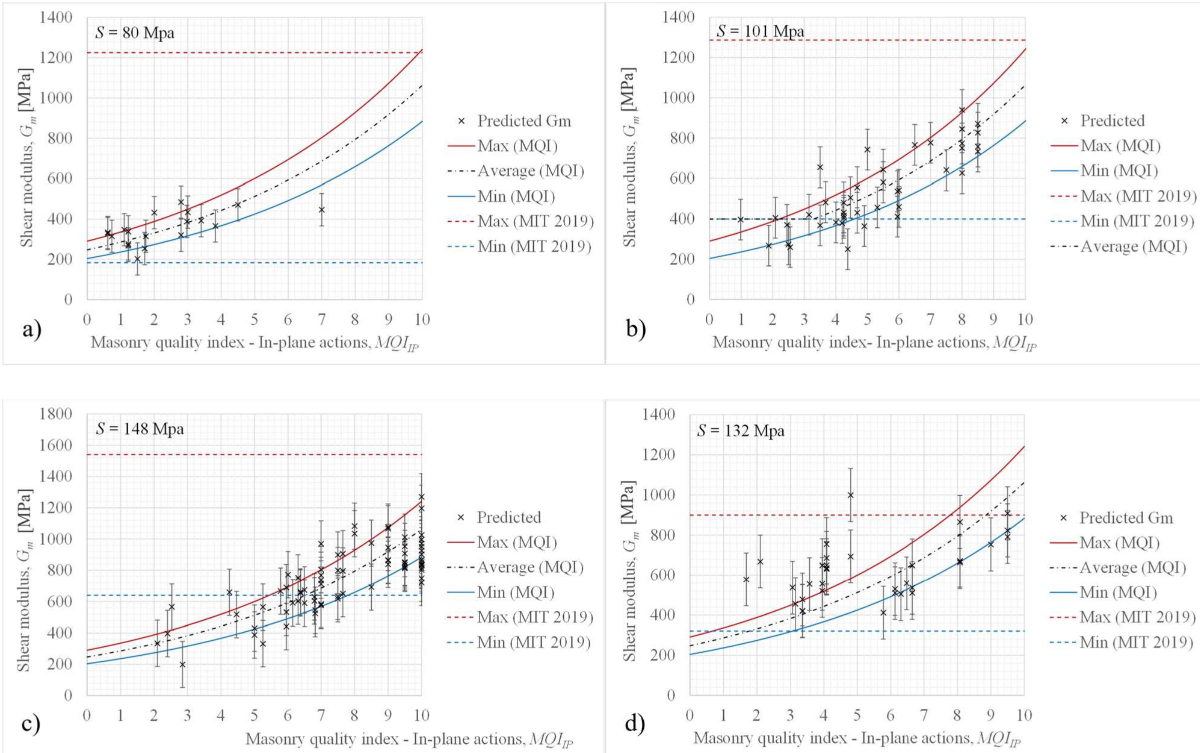

Figure 19 – The shear modulus, Gm, of the URM specimens grouped by URM type, and compared with masonry quality index for horizontal in-plane loading, MQII. a) irregular stone, with pebbles, erratic and irregular stone units; b) roughly cut stone with good bond; c) ashlar masonry with regular squared blocks and mortar joints; d) solid fired clay bricks with lime mortar.

The determined proportion coefficients for the shear modulus, K_{es}, were found to be in accordance with the values proposed by other sources, as shown in Table 13.

URM type	Proposed proportion coefficient for the shear modulus, K_{es}	K_{es} [60]	K_{es} [61]
Irregular stone, with pebbles, erratic and irregular stone units	0.322	0.4	0.45
Roughly cut stone with good bond	0.312		
Ashlar masonry with regular squared blocks and mortar joints	0.299		
Solid fired clay bricks with lime mortar	0.348		

Table 13 – Proposed shear modulus proportion coefficient, K_{es}, compared with other authors.

6. Comparison with Destructive Testing

Although it was not possible to extract any masonry prisms from the assessed churches due to heritage preservation constraints, the authors performed an experimental comparison between the proposed aggregated framework of procedures and the results of destructive testing performed in a controlled environment (i.e., in a laboratory) using masonry samples from another building wherein the expert judgment testing was carried out by the same lead researcher and the NDT techniques were executed using the same exact equipment as was used to assess the masonry materials in the Italian churches.

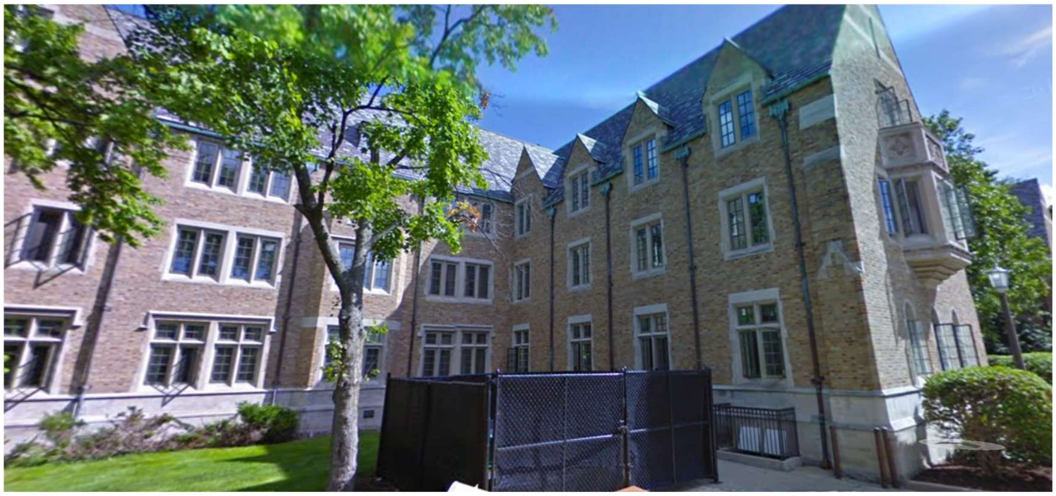

Figure 20 – Dillon Hall on the campus of the University of Notre Dame (Indiana,USA).

The comparison was based on a building located on the campus of the University of Notre Dame du Lac in Indiana, USA. Dillon Hall (Figure 20) is an approximately 100-years-old structure with URM infill walls and façade. Due to the renovation work the building was undergoing, it was possible to observe the unplastered texture of the URM walls and to apply all the NDT and expert judgment techniques as described in the current paper. Sixteen URM samples were tested in situ with the rebound hammer and pulse velocity instruments. Furthermore, given that the URM wall texture of Dillon Hall was categorized as "solid fire clay bricks with lime mortar", the related correlation coefficients of Table 9 were used in Equation 5 to determine the compressive strength, f'_m, as function of the determined mean rebound number, R, and mean indirect pulse velocity, v_i. The tested mean rebound number, R, mean indirect pulse velocity, v_i, and the calculated compressive strength, f'_m, are reported in Table 14.

URM sample	Mean rebound number, R	Mean indirect pulse velocity, v_i (m/s)	URM sample compressive strength, f'_m (MPa)
1	40.87	1504	4.90
2	41.33	1545	5.05
3	40.50	2792	6.95

URM sample	Mean rebound number, R	Mean indirect pulse velocity, v_i (m/s)	URM sample compressive strength, f'_m (MPa)
4	43.50	2656	7.32
5	42.88	2015	6.13
6	41.25	1786	5.48
7	44.80	2067	6.53
8	44.50	1536	5.46
9	44.88	1905	6.24
10	43.38	1771	5.76
11	45.75	1540	5.63
12	44.88	1432	5.29
13	45.75	1678	5.92
14	44.00	1636	5.59
15	44.63	1932	625
16	45.50	1798	6.13
Mean			**5.91**
Standard deviation			**0.64**
Coefficient of variation			**0.11**

Table 14 – Mean rebound number, R, mean indirect pulse velocity, v_i, and compressive strength, f'_m, of the URM samples tested in-situ.

Furthermore, sixteen brick samples and six URM prism samples were extracted from the walls and tested for compressive strength in the lab using a SATEC universal testing machine (Figure 21), in accordance with ASTM C67/C67M [51] and ASTM C1314 [62]. The results for the tested compressive strength of the brick and URM prism samples are given in Table 15 and Table 16, respectively.

Figure 21 – URM prisms extracted from the Dillon Hall.

Brick sample	Brick width, w_b (mm)	Brick thickness, t_b (mm)	Brick surface of loading, A_b (mm^2)	Peak load (N)	Brick compressive strength, f'_b (MPa)
1	90.49	100.01	9050	60718	6.71

Brick sample	Brick width, w_b (mm)	Brick thickness, t_b (mm)	Brick surface of loading, A_b (mm^2)	Peak load (N)	Brick compressive strength, f'_b (MPa)
2	101.60	96.84	9839	79450	8.08
3	100.02	92.08	9209	99885	10.85
4	92.87	101.60	9436	86740	9.19
5	96.84	93.67	9071	62589	6.90
6	101.60	89.70	9113	76685	8.41
7	96.05	101.60	9758	77850	7.98
8	101.60	96.05	9758	80574	8.26
9	102.39	91.28	9347	92921	9.94
10	96.05	100.01	9605	81139	8.45
11	94.46	88.90	8397	84142	10.02
12	91.29	102.40	9347	75675	8.10
13	100.02	96.05	9606	94498	9.84
14	96.84	100.01	9685	74786	7.72
15	94.46	102.40	9672	83800	8.66
16	85.73	93.67	8029	96328	12.00
Mean					**8.82**
Standard deviation					**1.37**
Coefficient of variation					**0.15**

Table 15 – Tested compressive strength of the brick samples, f'_b.

URM prism sample	URM prism width, w_p (mm)	URM prism thickness, t_p (mm)	URM prism height, h_p (mm)	URM prism surface of loading, A_p (mm^2)	Corrective factor due to h_p/t_p ratio	Peak load (N)	URM prism compressive strength, f'_m (MPa)
1	203.20	57.95	205.58	11774	1.114	50367	4.76
2	177.80	98.43	219.87	17500	1.019	55255	3.22
3	227.81	89.70	209.16	20433	1.027	103990	5.22
4	204.79	95.26	209.16	19507	1.016	82489	4.29
5	200.82	91.29	216.80	18332	1.030	100210	5.63
6	204.00	92.87	205.98	18945	1.017	105820	5.68
Mean							**4.80**
Standard deviation							**0.86**
Coefficient of variation							**0.18**

Table 16 – Tested compressive strength of the URM prism samples, f'_m .

Finally, the results for the compressive strength, f'_m, of both the lab-tested URM prisms (via destructive testing) and the in-situ tested URM samples (via aggregated NDT method) were normally distributed and compared in Figure 22. It might be noticed that the mean compressive strength determined in-situ is unconservatively overestimating the mean compressive strength determined for the lab-tested URM prisms by 23%.

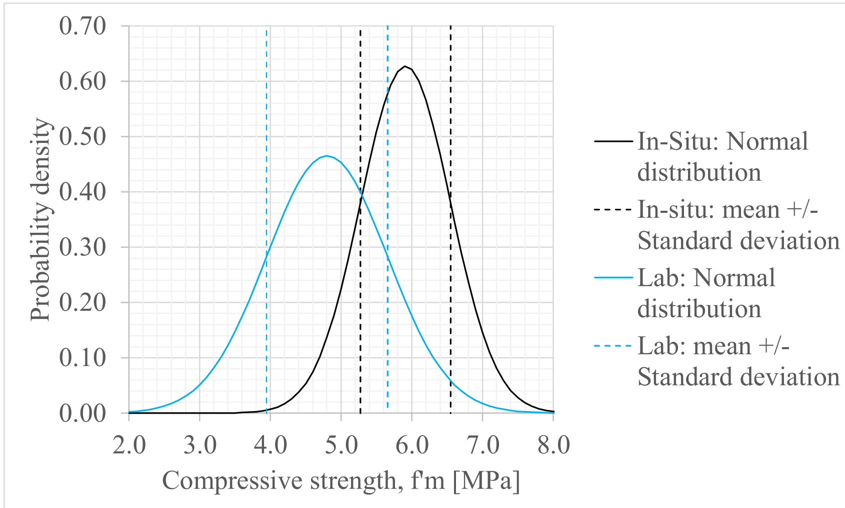

Figure 22 – Normal distribution of the compressive strength, f'_m, obtained from the sample tested in-situ via aggregated NDT method, and prism tested in lab via destructive testing.

To account for a conservative approach required for the application of the proposed procedure into real-world engineering assessment, approach A, as proposed by EN 13791:2007 [63], was used. In EN 13791:2019 [63], to determine the characteristic compressive strength, $f'_{m,k}$, a number k of standard deviations (depending on the number of tests performed) are to be subtracted from the mean compressive strength, f'_m, as shown in Equation 8. The proposed approach would result in a characteristic value corresponding to the 5th percentile of the compressive strength distribution for samples tested in-situ (Figure 22).

$$f'_{m,k} = f'_m - k(s) = 5.91 \text{ MPa} - 1.70(0.64 \text{ MPa}) = 4.82 \text{ MPa} \quad (8)$$

where: f'_m is the mean compressive strength of the masonry (as shown in Table 14 for this example);

k is depending on the number of tests performed ($k = 1.70$ for 16 tests); and

s is the standard deviation (as shown in Table 14 for this example).

Although the different age and material might have affected the application of the proposed procedure on the Dillon Hall samples, it might be noticed that the characteristic compressive strength, $f'_{m,k}$, determined via the proposed aggregated NDT method on the in-situ samples is estimating the mean compressive strength determined from the lab-tested URM prisms with an approximation of 0.4%. A similar approach was applied to Equation 5 to determine a more conservative characteristic compressive strength when the proposed aggregated NDT method is applied. Hence, Equation 5 was modified into Equation 9.

$$f'_{m,k} = a{v_i}^b R^c - k(s) \tag{9}$$

Nonetheless, the authors also acknowledge the significant difference between the historic URM tested to develop the proposed aggregated NDT method and the lab-tested relatively modern URM samples, as well as the limitations of the sample size used for the partial validation, hence, they suggest interpreting the results cautiously and encourage further testing on a more various array of materials to validate Equation 9.

7. Summary, Conclusions, and Further Research

In the current research, 170 URM specimens belonging to 72 URM Italian medieval churches were investigated using two expert judgment approaches (i.e., MQI and MIT2019) and two NDT techniques (i.e., rebound hammer test, and pulse velocity test). The results of the investigation techniques were aggregated to develop a more comprehensive non-destructive methodology to assess the mechanical properties of the URM (i.e., compressive strength, Young's modulus, and shear modulus) based on the procedure known as "SonReb". In fact, the deficiencies of particular techniques were often offset by aggregating the results with other techniques as proposed herein and as extensively discussed in Table 2.

The results were also founded to be in agreement with the findings of previous studies based on semi-destructive and destructive assessment techniques [56, 60, 58, 61, 59, 57]. Although the authors are aware that destructive tests are preferable for achieving more reliable results, the proposed methodology might be potentially useful for all those situations in which, for any given reason, only NDT techniques are feasible.

Solely a partial validation on a more modern building was possible through destructive testing due to architectural and historical constraints acting on the studied churches, however, the results of the proposed methodology were found to be relatively close to the ones obtained via laboratory testing. The typical "SonReb" formulation (Equation 5), was adjusted in a conservative manner to account for the larger variability of URM when compared with concrete (Equation 9). The authors are aware that the described validation is merely partial because of the limited sample size and URM types that have been lab-tested, therefore, a proper correlation among the predicted compressive strength and the lab-tested one could not be performed. The authors also acknowledge the significant difference between the historic URM tested to develop the proposed aggregated NDT method and the lab-tested relatively modern URM samples, hence, they suggest interpreting the results cautiously and encourage further testing to validate the proposed equations.

The proposed aggregated technique could be applied to improve previously developed qualitative risk assessment methods (e.g., Pirchio, et al. [15]), in fact, the robustness of at least 20 out of 28 collapse mechanisms (roughly 23%) identified for the macro-blocks approach for determining the vulnerability of URM churches are directly affected by the quality of the composing URM materials [38, 39]. Furthermore, the determined mechanical properties were further used to develop complete structural building information models (BIM) of a selected case study church, and to achieve an exhaustive structural analysis to compare the results of the detailed analysis with the results of previous assessments [64].

Acknowledgments

This research was primarily funded by a Global Gateways Faculty Research Award at the University of Notre Dame (grant FY18RGG03). Undergraduate students at the University of Notre Dame who assisted with the surveys include Elizabeth DePaola, Emily Brady, Lily Polster, Marie Bond, and Patricia Dirlam. These students were supported by research scholarship funding from various programs, institutes, and centers at the University of Notre Dame, including the Fitzgerald Institute for Real Estate, the Grand Challenges Scholars Program, the Women in Engineering Program, and the Flatley Center for Undergraduate Scholarly Engagement.

The authors are thankful for the assistance of the cultural heritage offices of the involved dioceses, as well as the assistance of Dr. Federica Romiti (diocese of Anagni – Alatri), Bishop Stefano Manetti and Surveyor Marco Cortellessa (diocese of Montepulciano – Chiusi – Pienza), Don Francesco Valentini and Dr. Giovanna Bandinu (diocese of Orvieto – Todi), Arch. Agapito Fornari (diocese of Palestrina), Don Riccardo Pascolini (diocese of Perugia – Città della Pieve), Don Fabio Sottoriva (diocese of Vicenza), Dr. Monia Sartori (archdiocese of Trento), Arch. Graziana Santamaria, and Surveyor Marco Cherubini. The first author would like to thank his parents Valter Pirchio and Lorena Trentini for their assistance with logistics, as well as an undergraduate student at the University of Trento, Chiara Meloni. The following priests are thanked for granting access to their churches and for assisting during the data collection:

- Diocese of Anagni – Alatri: Deacon Massimiliano Floridi, Don Alessandro De Sanctis, Don Antonio Castagnacci, Don Pierino Giacomi, Don Roberto Martufi, Don Virginio De Rocchis, and the parishes' collaborators.
- Diocese of Montepulciano – Chiusi – Pienza: Don Andrea Malacarne, Don Antonio Nutarelli, Don Azelio Mariani, Don Carlo Sensani, Don Elia Sartori, Don Francesco Monachini, Don Kishor Uppalapati, Don Manlio Sodi, Don Sergio Graziani, Don Silvano Nardi, Don Stefano Cinelli, and the parishes' collaborators.
- Diocese of Nocera Inferiore – Sarno: Friar Damiano Antonino, Friar Felice Petrone, Friar Michele Alfano, Friar Raffaele Panopio, Friar Renato Sapere, and the parishes' collaborators.
- Diocese of Orvieto – Todi: Don Claudio Calzoli, Don Jeremiah Joseph Kelly, Don Marcello Sargeni, Don Marco Gasparri, Don Piero Grassi, and Don Zeffiro Tordi.
- Diocese of Palestrina: Monsignor Andrea Lonardo (diocese of Rome), Don Davide Maria Martinelli, and the parishes' collaborators.

- Diocese of Perugia – Città della Pieve: Don Augusto Martelli, Don Fabio Quaresima, Don Gianni Pollini, Don Giuseppe Piccioni, Don Marco Merlini, Don Matteo Rubechini, Don Vincenzo Esposito, and the parishes' collaborators.
- Diocese of Sorrento – Castellammare di Stabia: Don Antonino Lazzazzara, Don Beniamino Di Martino, Don Ciro Esposito, Don Maurizio Esposito, and the parishes' collaborators.
- Diocese of Trento: Don Ferdinando Murari, Don Maurizio Toldo, and the parishes' collaborators.
- Diocese of Vicenza: Don Adriano Preto Martini, Don Fabio Ogliani, Don Francesco Strazzari, Don Giacomo Viali, Don Giovanni Campagnolo, Don Giovanni Imbonati, Don Giovanni Sandonà, Don Giuseppe Mattiello, Don Luigi Spadetto, Don Paolo Zampiva, and the parishes' collaborators.

References

[1] B. Galliani, Dell'Architettura, Libri Dieci di M.Vitruvio Pollione, Milano: A. Dozio, 1832.

[2] C. Gloria, "Evoluzione storica dei leganti e dei conglomerati: dall'empirismo alla loro conoscenza razionale," in *Cemento: Storia, Tecnologia, Applicazioni*, Fratelli Fabri Editori, 1976.

[3] J. P. Adam, L'arte di costruire presso i Romani: materiali e tecniche, Longanesi: Milano, 1984.

[4] S. Di Pasquale, L'arte del costruire: tra conoscenza e scienza., Venezia: Marsilio, 1996.

[5] A. Cagnana, "La transizione al Medioevo attraverso la storia delle tecniche murarie: dall'analisi di un territorio ad un problema sovraregionale," in *I Congresso Nazionale di Archeologia Medievale*, Pisa, 1997.

[6] F. Doglioni, A. Moretti and V. Petrini, Le chiese e il terremoto. Dalla vulnerabilità constatata nel terremoto del Friuli al miglioramento antisismico nel restauro. Verso una politica di prevenzione., Trieste: Edizioni Lint, 1994.

[7] G. Proietti, "Dopo la polvere". Rilevazione degli interventi di recupero (1985-1989) del patrimoni artistico-monumentale danneggiato dal terremoto del 1980-1981, Roma: Istituto Poligrafico e Zecca dello Stato, 1994.

[8] S. Lagomarsino, A. Brencich, F. Bussolino, A. Moretti, L. C. Pagnini and S. Podestà, "Una nuova metodologia per il rilievo del danno alle chiese: prime considerazioni sui meccanismi attivati dal sisma.," *Ingegneria Sismica,* vol. 14, no. 3, pp. 70-82, 1997.

[9] F. Doglioni, "Codice di pratica (Linee Guida) per la progettazione degli interventi di riparazione, miglioramento sismico e restauro dei beni architettonici danneggiati dal terremoto umbro-marchigiano del 1997," *Bollettino Ufficiale Regione Marche,* vol. 15, 2000.

[10] S. Lagomarsino and S. Podestà, "Damage and vulnerability assessment of churches after the 2002 Molise, Italy, earthquake.," *Earthquake Spectra,* vol. 20, no. S1, pp. S271-S283, 2004.

[11] G. P. Cimellaro, I. P. Christovasilis, A. M. Reinhorn, A. De Stefano and T. Kirova, "L'Aquila Earthquake of April 6, 2009 in Italy: Rebuilding a Resilient City to Withstand Multiple Hazards," MCEER, 2010.

[12] F. da Porto, B. Silva, C. Costa and C. Modena, "Macro-scale analysis of damage to churches after earthquake in Abruzzo (Italy) on April 6, 2009," *Journal of Earthquake Engineering,* vol. 16, no. 6, pp. 739-758, 2012.

[13] L. Liberatore, L. D. Decanini and D. Liberatore, "The performance of churches in the 2012 Emilia earthquakes.," *Bulletin of Earthquake Engineering,* vol. 12, no. 5, pp. 2299-2331, 2014.

[14] A. Penna, C. Calderini, L. Sorrentino, C. F. Carocci, E. Cescatti, R. Sisti, A. Borri, C. Modena and A. Prota, "Damage to churches in the 2016 central Italy earthquakes," *Bulletin of Earthquake Engineering,* vol. 17, no. 10, pp. 1-28, 2019.

[15] D. Pirchio, K. Q. Walsh, E. Kerr, I. Giongo, M. Giaretton, L. Sorrentino, B. D. Weldon and L. Ciocci, "Seismic risk assessment and intervention prioritization for Italian medieval churches," *Journal of Building Engineering,* vol. 43, no. 103061, 2021.

[16] B. Quelhas, L. Cantini, J. M. Guedes, F. da Porto and C. Almeida, "Characterization and reinforcement of stone masonry walls," *In Structural Rehabilitation of Old Buildings,* pp. 131-155, 2014.

[17] D. P. Abrams, O. AlShawa, P. B. Lourenço and L. Sorrentino, "Out-of-Plane Seismic Response of Unreinforced Masonry Walls: Conceptual Discussion, Research Needs, and Modeling Issues.," *International Journal of Architectural Heritage,* vol. 11, no. 1, pp. 22-30, 2017.

[18] K. Q. Walsh, D. Y. Dizhur, I. Giongo, H. Derakhshan and J. M. Ingham, "Effect of boundary conditions and other factors on URM wall out-of-plane behaviour: design demands, predicted capacity, and in situ proof test results," *Sesoc Journal,* vol. 30, no. 1, p. 57, 2017.

[19] A. Pir, L. S. Hogan, D. Y. Dizhur, K. Q. Walsh and J. M. Ingham, "A comparison of numerically and experimentally obtained in-plane responses of a full-scale unreinforced masonry building frame," in *Tenth Pacific Conference on Earthquake*, Auckland, 2015.

[20] S. Lopez, M. D'Amato, L. Ramos, M. Laterza and P. B. Lourenço, "Simplified formulations for estimating the main frequencies of ancient masonry churches.," *Frontiers in Built Environment,* vol. 5, pp. 18.1-18.15, 2019.

[21] D. M. McCann and M. C. Forde, "Review of NDT methods in the assessment of concrete and masonry structures," *NDT & E International,* vol. 34, no. 2, pp. 71-84, 2001.

[22] L. Binda, M. Lualdi and A. Saisi, "Non-destructive testing techniques applied for diagnostic investigation: Syracuse Cathedral in Sicily, Italy.," *International Journal of Architectural Heritage,* vol. 1, no. 4, pp. 380-402, 2007.

[23] V. Bosiljkov, V. Bokan-Bosiljkov, B. Strah, J. Velkavrh and P. Cotič, "Review of innovative techniques for the knowledge of cultural assets. PERPETUATE Project, Deliverable D, 6.," PERPETUATE Project, 2010.

[24] M. C. Forde, "International practice using NDE for the inspection of concrete and masonry arch bridges.," *Bridge Structures,* vol. 6, no. 1, 2, pp. 25-34, 2010.

[25] M. Andreini, A. De Falco, L. Giresini and M. Sassu, "Mechanical characterization of masonry walls with chaotic texture: Procedures and results of in-situ tests.," *International Journal of Architectural Heritage,* vol. 8, no. 3, pp. 376-407, 2014.

[26] M. Roknuzzaman, M. B. Hossain, M. I. Mostazid and M. R. Haque, "Application of rebound hammer method for estimating compressive strength of bricks," *Journal of Civil Engineering Research,* vol. 7, no. 3, pp. 99-104, 2017.

[27] M. Arduini, A. Di Leo and G. Pascale, "Experimental methods for on site evaluation of the mechanical properties of masonry," in *Tenth International Brick & Block Masonry Conference*, Alberta, 1994.

[28] B. Conde, L. F. Ramos, D. V. Oliveira, B. Riveiro and M. Solla, "Structural assessment of masonry arch bridges by combination of non-destructive testing techniques and three-dimensional numerical modelling: Application to Vilanova bridge," *Engineering Structures,* vol. 148, pp. 621-638, 2017.

[29] R. Martini, J. Carvalho, N. Barraca, A. Arêde and H. Varum, "Advances on the use of non-destructive techniques for mechanical characterization of stone masonry: GPR and sonic tests.," *Procedia Structural Integrity,* vol. 5, pp. 1108-1115, 2017.

[30] M. R. Valluzzi, E. Cescatti, G. Cardani, L. Cantini, L. Zanzi, C. Colla and F. Casarin, "Calibration of sonic pulse velocity tests for detection of variable conditions in masonry walls.," *Construction and Building Materials,* vol. 192, pp. 272-286, 2018.

[31] MIT, *Norme Tecniche per le Costruzioni,* Roma: Ministero delle Infrastrutture e dei Trasporti (MIT), 2018.

[32] MIT, *Commentario alle Norme Tecniche dell Costruzioni,* Roma: Ministero delle Infrastrutture e dei Trasporti (MIT), 2019.

[33] A. Borri and A. De Maria, "Il metodo IQM per la stima delle caratteristiche meccaniche delle murature: allineamento alla circolare n. 7/2019.," *ANIDIS,* pp. 2-21, 2019.

[34] M. Marino, F. Neri, A. Borri and A. De Maria, “Experimental data of friction coefficient for some types of masonry and its correlation with an index of quality of Masonry (IQM),” in

Proceedings of the 2nd European conference on earthquake engineering and seismology, Istanbul, 2014.

[35] J. Gasparik, *Prove non distruttive nell'edilizia,* Brescia: Associazione Italiana Prove non Distruttive, 1992.

[36] A. Di Leo and G. Pascale, "Prove non distruttive sulle costruzioni in cemento armato," *Il Giornale delle Prove non Distruttive Monitoraggio Diagnostica,* vol. 4, 1994.

[37] RILEM, "NDT 4 Recommendation for in situ concrete strength determination by combined non-destructive methods, 1993," in *RILEM Recommendations for the Testing and Use of Constructions Materials*, E & FN SPON, 1994, pp. 92-98.

[38] D.P.C.M. 9 febbraio, *Valutazione e riduzione del rischio sismico del patrimonio culturale con riferimento alle Norme tecniche per le costruzioni di cui al D.M. 14/01/2008,* 2011.

[39] A. Marotta, S. Sorrentino, D. Liberatore and J. M. Ingham, "Vulnerability Assessment of Unreinforced Masonry Churches Following the 2010-2011 Canterbury Earthquake Sequence," *Journal of Earthquake Engineering,* vol. 21, no. 6, pp. 912-934, 2017.

[40] F. Gàlvez, S. R. Abeling, K. Ip, S. Giovinazzi, D. Dizhur and J. M. Ingham, "Using the Macro-element Method to Seismically Assess Complex URM Buildings," in *10th Australian Masonry Conference*, Sydney, 2018.

[41] A. Borri, M. Corradi, G. Castori and A. De Maria, "A method for the analysis and classification of historic masonry," *Bulletin of Earthquake Engineering,* vol. 13, no. 9, pp. 2647-2665, 2015.

[42] A. Masi, "La stima della resistenza del calcestruzzo in situ mediante prove distruttive e non distruttive," *Il Giornale delle Prove non Distruttive Monitoraggio Diagnostica,* vol. 1, 2005.

[43] G. Vasconcelos, P. B. Lourenço, C. A. Alves and J. Pamplona, "Prediction of the mechanical properties of granites by ultrasonic pulse velocity and Schmidt hammer hardness.," *Ultrasonics,* vol. 48, no. 5, pp. 453-466, 2008.

[44] E. Vasanelli, A. Calia, D. Colangiuli, F. Micelli and M. A. Aiello, "Assessing the reliability of non-destructive and moderately invasive techniques for the evaluation of uniaxial compressive strength of stone masonry units.," *Construction and Building Materials,* vol. 124, pp. 575-581, 2016.

[45] American Society for Testing and Materials, *ASTM C805/C805M,* US: ASTM International, 2018.

[46] Euorpean Committee for Standardization, *EN 12504-2:2012,* Euorpean Committee for Standardization, 2012.

[47] V. A. M. Luprano and C. Colla, "Ultrasonic and sonic techniques applied to concrete and masonry structures.," *Recent Advances in Non-Destructive Inspections,* pp. 59-88, 2011.

[48] R. Martini, J. Carvalho, N. Barraca, A. Arêde and H. Varum, "Advances on the use of non-destructive techniques for mechanical characterization of stone masonry: GPR and sonic tests.," *Procedia Structural Integrity,* vol. 5, pp. 1108-1115, 2017.

[49] American Society for Testing and Materials, *ASTM C597,* US: ASTM Internationl, 2016.

[50] Euorpean Committee for Standardization, *EN 12504-4:2005,* Euorpean Committee for Standardization, 2005.

[51] American Society for Testing and Materials, *ASTM C67/C67M,* US: ASTM International, 2018.

[52] J. T. Petro Jr and J. Kim, "Detection of delamination in concrete using ultrasonic pulse velocity test.," *Construction and Building Materials,* vol. 26, no. 1, pp. 574-582, 2012.

[53] L. Nobile and M. Bonagura, "Accuracy of non-destructive evaluation of concrete compression strength," in *The 12th International Conference of the Slovenian Society for Non-Destructive Testing*, Portorož, 2013.

[54] A. A. E. Aliabdo and A. E. M. A. Elmoaty, "Reliability of using nondestructive tests to estimate compressive strength of building stones and bricks.," *Alexandria Engineering Journal,* vol. 51, no. 3, pp. 193 - 203, 2012.

[55] J. Brozovskj, "Determine the compressive strength of calcium silicate bricks by combined nondestructive method.," *The Scientific World Journal,* 2014.

[56] Federal Emergency Management Agency, *FEMA 306,* Redwood City: Applied Technology Council (ATC-43 Project), 1999.

[57] New Zealand Society for Earthquake Engineering and Structural Engineering Society New Zealand, *NZSEE,* NZSEE, 2016.

[58] R. Drysdale, A. Hamid and L. Baker, Masonry Structures: Behavior and Design, Boulder, Colorado: The Masonry Society , 1999.

[59] H. B. Kaushik, D. C. Rai and S. K. Jain, "Stress-strain characteristics of clay brick masonry under uniaxial compression," *Journal of Materials in Civil Engineering,* vol. 19, no. 9, pp. 728-739, 2007.

[60] Euorpean Committee for Standardization, *EN 1996-1-1:2006,* Brussels: Euorpean Committee for Standardization, 2006.

[61] V. Z. Bosiljkov, Y. Z. Totoev and J. M. Nichols, "Shear modulus and stiffness of brickwork masonry: an experimental perspective," *Structural Engineering and Mechanics,* vol. 20, no. 1, pp. 21-44, 2005.

[62] American Society for Testing and Materials, *ASTM C1314,* US: ASTM International, 2018.

[63] European Committee for Standardization, *EN 13971:2019,* Brussells: European Committee for Standardization, 2019.

[64] D. Pirchio, K. Q. Walsh, E. Kerr, M. Giongo, B. D. Weldon, L. Ciocci and L. Sorrentino, "Integrated framework to structurally model unreinforced masonry Italian medieval churches from photogrammetry to finite element model analysis through heritage building information modeling," *Engineering Structures,* vol. 241, no. 112439, 2021.

[65] T. Narendra, Design of reinforced masonry structures, McGraw-Hill, 2010.

[66] S. Lagomarsino, "Damage assessment of churches after l'Aquila earthquake (2009)," *Bulletin of Earthquake Engineering,* vol. 10, no. 1, pp. 73-92, 2012.

[67] F. Aydın and M. Saribiyik, "Correlation between Schmidt Hammer and destructive compressions testing for concretes in existing buildings," *Scientific Research and Essays,* vol. 5, no. 13, pp. 1644-1648, 2010.

[68] N. Makoond, L. Pelà and C. Molins, "Dynamic elastic properties of brick masonry constituents," *Construction and Building Materials,* vol. 199, pp. 756-770, 2019.

[69] J. Brozovsky, "Use of non-destructive ultrasonic pulse testing methods in evaluation of brick parameters," in *Proceedings of the 3rd International Conference on Sustainable Construction Materials & Technologies (SCMT'13)*, 2013.

[70] V. Brotons, R. Tomás, S. Ivorra and A. Grediaga, "Relationship between static and dynamic elastic modulus of calcarenite heated at different temperatures: the San Julián's stone," *Bulletin of Engineering Geology and the Environment,* vol. 73, no. 3, pp. 791-799, 2014.

[71] M. Ohtsu, "Innovative AE and NDT techniques for on-site measurement of concrete and masonry structures," *RILEM State-of-the-Art Reports,* vol. 20, pp. 89-103, 2016.

[72] J. Bakhteri, A. M. Makhtar and S. Sambasivam, "Finite element modelling of structural clay brick masonry subjected to axial compression," *Jurnal Teknologi,* vol. 41, no. 1, pp. 57-68, 2004.

[73] J. Middleton, G. N. Pande and B. Kralj, "Computer Methods in Structural Masonry-4," in *Proceedings of the Fourth International Symposium on Computer Methods in Structural Masonry*, London, 1998.

[74] H. A. Harris, Masonry: Materials, design, construction, and maintenance, ASTM International, 1988.

[75] A. J. Francis, C. B. Horman and L. E. Jerrems, "The effect of joint thickness and other factors on the compressive strength of brickwork," in *Proceedings of the second international brick masonry conference*, 1971.

Index of the Figures

Index of the Tables

741 Appendix A – Selected Churches

#	Church Name	Region	Diocese	Settlement / City	Coordinates WGS84 GD	Role	Original Construction Year
1	Santi Dioniso, Rustico ed Eleuterio Martiri	Trentino – Alto Adige	Trento	Santa Croce	46.066530 10.839030	Parish church	1155
2	Santa Maria Assunta	Trentino – Alto Adige	Trento	Tavodo	46.066530 10.893080	Parish church	1160
3	San Giovanni Apostolo ed Evangelista	Trentino – Alto Adige	Trento	Poia	46.028870 10.884130	Parish church	1200
4	San Marcello	Trentino – Alto Adige	Trento	Lundo	46.011910 10.884130	Parish church	1200
5	Santa Maria Assunta	Trentino – Alto Adige	Trento	Dasindo	46.010960 10.860530	Subsidiary church	1200
6	San Lorenzo	Trentino – Alto Adige	Trento	Vigo Lomaso	46.012050 10.872040	Parish church	1210
7	San Nicolò	Trentino – Alto Adige	Trento	Comighello	46.034260 10.849410	Parish church	1250
8	Santa Maria Assunta e San Giovanni Battista	Trentino – Alto Adige	Trento	Tione	46.034190 10.729450	Parish church	1300
9	Annunciazione di Maria	Trentino – Alto Adige	Trento	Rango	46.018330 10.811640	Parish church	1400
10	San Felice	Trentino – Alto Adige	Trento	Bono	46.026080 10.848670	Parish church	1480
11	Santi Pietro e Paolo	Trentino – Alto Adige	Trento	Sclemo	46.055610 10.882940	Subsidiary church	1490
12	San Vigilio	Trentino – Alto Adige	Trento	Stenico	46.052460 10.854170	Parish church	1500
13	San Giorgio	Trentino – Alto Adige	Trento	Dorsino	46.072690 10.896920	Subsidiary church	1500
14	Santi Pietro e Paolo	Trentino – Alto Adige	Trento	Cares	46.032700 10.866660	Parish church	1500
15	San Biagio Vescovo e Martire	Trentino – Alto Adige	Trento	Favrio	45.999920 10.858800	Subsidiary church	1500
16	Sant'Antonio Abate	Trentino – Alto Adige	Trento	Bivedo	46.028170 10.827460	Parish church	1530[2]
17	Immacolata e Santi Fabiano e Sebastiano	Trentino – Alto Adige	Trento	Fiavè	46.004600 10.842050	Parish church	1540 (1880)[1]
18	Santa Maria Etiopissa	Veneto	Vicenza	Polegge	45.605930 11.557180	Subsidiary church	1000
19	Santa Maria e Santa Fosca	Veneto	Vicenza	Dueville	45.634970 11.548010	Parish church	1050 (1955)[1]
20	Santa Maria Annunziata	Veneto	Vicenza	Poia	45.530100 11.423720	Parish church	1300
21	San Pietro Apostolo	Veneto	Vicenza	Monticello Conte Otto	45.594130 11.585370	Parish church	1350
22	Santa Margherita Vergine e Martire	Veneto	Vicenza	Posina	45.790430 11.261480	Parish church	1400
23	Santissima Trinità	Veneto	Vicenza	Bassano del Grappa	45.724970 11.721980	Parish church	1400
24	Santi Pietro e Paolo	Veneto	Vicenza	Nove	45.724970 11.680790	Parish church	1440

#	Church Name	Region	Diocese	Settlement / City	Coordinates WGS84 GD	Role	Original Construction Year
25	Santi Girolamo e Bernardino	Veneto	Vicenza	Vivaro	45.610720 11.544320	Parish church	1460
26	Santo Stefano Protomartire	Veneto	Vicenza	Lupia	45.640930 11.608730	Parish church	1470
27	San Matteo Apostolo	Veneto	Vicenza	Cavazzale	45.600760 11.569250	Parish church	1480
28	San Michele Arcangelo	Veneto	Vicenza	Sarmego	45.599800 11.671670	Parish church	1500
29	Santa Cristina	Veneto	Vicenza	Poianella	45.632870 11.625320	Parish church	1560[2]
30	Beata Vergine di Monte Berico	Veneto	Vicenza	Vivaro	45.621370 11.560270	Subsidiary church	1770[1]
31	San Secondiano	Toscana	Montepulciano – Chiusi - Pienza	Chiusi	43.015560 11.949120	Parish church	550[1]
32	San Lorenzo	Toscana	Montepulciano – Chiusi - Pienza	Valiano	43.148320 11.901600	Parish church	1100
33	Santa Croce	Toscana	Montepulciano – Chiusi - Pienza	Abbadia San Salvatore	42.880090 11.678360	Parish church	1100
34	Santi Pietro e Paolo	Toscana	Montepulciano – Chiusi - Pienza	Petroio	43.141490 11.688210	Parish church	1180
35	Santi Leonardo e Cassiano	Toscana	Montepulciano – Chiusi - Pienza	San Casciano dei Bagni	42.871630 11.875230	Parish church	1200
36	Santissima Annunziata	Toscana	Montepulciano – Chiusi - Pienza	Montisi	43.156690 11.651720	Parish church	1200
37	San Francesco	Toscana	Montepulciano – Chiusi - Pienza	Chiusi	43.016640 11.947110	Parish church	1210
38	San Leonardo	Toscana	Montepulciano – Chiusi - Pienza	Montefollonico	43.128120 11.745330	Parish church	1215
39	San Pietro	Toscana	Montepulciano – Chiusi - Pienza	Radicofani	42.896360 11.767490	Parish church	1220
40	Santi Leonardo e Cristoforo	Toscana	Montepulciano – Chiusi - Pienza	Monticchiello	43.068370 11.725680	Parish church	1300
41	Sant'Apollinar e	Toscana	Montepulciano – Chiusi - Pienza	San Francesco	43.016000 11.946030	Subsidiary church	1400
42	San Vincenzo e Anasiasio	Toscana	Montepulciano – Chiusi - Pienza	Ascianello	43.139580 11.797180	Subsidiary church	1450
43	San Giovanni Battista	Umbria	Perugia – Città della Pieve	Castiglione della Valle	43.018110 12.253970	Parish church	1100
44	San Feliciano	Umbria	Perugia – Città della Pieve	San Feliciano	43.119030 12.166770	Parish church	1170
45	Sant'Ansano Martire	Umbria	Perugia – Città della Pieve	Petrignano del Lago	43.148450 11.937900	Parish church	1190
46	Crocifisso	Umbria	Perugia – Città della Pieve	Torgiano	43.018380 12.437670	Parish church	1200
47	San Martino di Fontana	Umbria	Perugia – Città della Pieve	Fontana	43.113110 12.324470	Parish church	1300
48	Santissimo Salvatore e Santa Maria Assunta	Umbria	Perugia – Città della Pieve	Paciano	43.023420 12.070170	Parish church	1480
49	San Lorenzo	Umbria	Perugia – Città della Pieve	Gioiella	43.093580 11.971890	Parish church	1500
50	Santa Maria delle Grazie	Umbria	Perugia – Città della Pieve	Montepetriolo	43.016910 12.229730	Subsidiary church	1500
51	Annunziata	Umbria	Perugia – Città della Pieve	Fontignano	43.026540 12.191760	Subsidiary church	1500

#	Church Name	Region	Diocese	Settlement / City	Coordinates WGS84 GD	Role	Original Construction Year
52	San Terenziano	Umbria	Orvieto - Todi	San Terenziano	42.863510 12.471800	Parish church	1200
53	Santi Giacomo e Marco	Umbria	Orvieto - Todi	Castel dell'Aquila	42.633830 12.406490	Parish church	1200
54	San Lorenzo Martire	Umbria	Orvieto - Todi	Montegiove	42.917050 12.144030	Subsidiary church	1270
55	San Biagio Vescovo e Martire	Umbria	Orvieto - Todi	Porano	42.686550 12.101730	Parish church	1270
56	Sant'Andrea Apostolo	Umbria	Orvieto - Todi	Marcellano	42.872980 12.520790	Parish church	1300
57	Santa Maria Assunta	Umbria	Orvieto - Todi	Montecchio	42.663140 12.286270	Parish church	1300
58	San Nicolò	Umbria	Orvieto - Todi	Farnetta	42.648420 12.453280	Parish church	1400
59	San Pancrazio Martire	Umbria	Orvieto - Todi	Castel Giorgio	42.704710 11.979650	Parish church	1520[2]
60	Maddalena	Lazio	Anagni-Alatri	Alatri	41.716550 13.352380	Subsidiary church	1100
61	Santa Maria Maggiore	Lazio	Anagni Alatri	Alatri	41.726150 13.342160	Parish church	1100
62	Santa Maria al Colle	Lazio	Anagni Alatri	Fiuggi	41.804120 13.218100	Parish church	1200
63	Santi Nicola e Giovanni	Lazio	Anagni Alatri	Filettino	41.889500 13.319210	Subsidiary church	1200
64	Sant'Antonio	Lazio	Anagni Alatri	Filettino	41.890270 13.328870	Subsidiary church	1274
65	San Michele Arcangelo e San Gaurico	Lazio	Anagni Alatri	Fumone	41.727160 13.290440	Parish church	1350
66	Santa Maria Maddalena	Lazio	Palestrina	Capranica Prenestina	41.862310 12.952400	Parish church	1400
67	Santissima Annunziata	Campania	Sorrento – Castellammare di Stabia	Vico Equense	40.663880 14.423930	Subsidiary church	1330
68	San Renato Vescovo	Campania	Sorrento – Castellammare di Stabia	Moiano	40.650660 14.466020	Parish church	1340
69	Santa Maria Assunta	Campania	Sorrento – Castellammare di Stabia	Vico Equense	40.655540 14.435040	Subsidiary church	1400
70	Santa Maria di Casarlano	Campania	Sorrento – Castellammare di Stabia	Casarlano	40.623250 14.391680	Parish church	1425
71	San Giovanni Evangelista	Campania	Sorrento – Castellammare di Stabia	Vico Equense	40.662960 14.436400	Parish church	1490
72	Sant'Antonio	Campania	Nocera Inferiore - Sarno	Nocera Inferiore	40.746980 14.645720	Parish church	1260

[1]The church was selected beyond specific request of the diocese.

[2]Although the original construction year is slightly outside of the selected limits, the church was selected because it was respecting the other criteria.

Table A 1 – Selected churches.

Appendix B – Collected Data for each NDT

URM type: Rubble stones						
Specimen #	**Church #**	**Macro-block**	**Masonry quality index – Vertical actions, (MQI_V)**	**Masonry quality index – In-plane horizontal actions, (MQI_I)**	**Pulse indirect velocity, v_i [m/s]**	**Rebound number, R**
1	8	Bell Tower	5.950	5.950	975.000	39.000
2	18	Facade	0.250	0.500	959.600	44.308
3	31	Lateral Wall	2.100	1.750	1691.800	25.625
4	34	Apse	1.225	1.050	1846.600	30.313
5		Bell Tower	1.050	1.225	1149.400	32.813
6	36	Lateral Wall	1.750	1.575	2010.333	33.625
7	43	Lateral Wall	2.975	3.400	1496.667	38.375
8		Apse	2.450	2.800	1241.250	31.000
9	44	Lateral Wall	3.150	2.450	1070.250	24.250
10		Bell Tower	2.975	3.825	1223.333	35.750
11	47	Bell Tower	4.500	4.500	2754.333	46.313
12	55	Bell Tower	1.750	1.750	1696.250	30.313
13	56	Facade	3.188	2.975	1639.400	37.938
14		Lateral Wall	3.500	3.000	1847.333	42.750
15	62	Lateral Wall	2.000	2.000	1005.500	42.750
16	65	Lateral Wall	6.500	6.000	2234.250	47.875
17	66	Bell Tower	1.125	1.225	1053.667	26.563
18	67	Apse	1.500	1.500	750.333	19.125
19	69	Facade	1.050	0.875	999.750	31.875
20		Lateral Wall	1.050	0.875	1237.333	32.375

Table B 1 – Collected data for 20 URM specimens for URM type: rubble stones.

URM type: split stones with good texture						
Specimen #	**Church #**	**Macroblock**	**Masonry quality index – Vertical actions, (MQI_V)**	**Masonry quality index – In-plane horizontal actions, (MQI_{IP})**	**Pulse indirect velocity, v_i [m/s]**	**Rebound number, R**
1	5	Bell Tower	5.100	5.313	1392.000	38.875

URM type: split stones with good texture						
Specimen #	**Church #**	**Macroblock**	**Masonry quality index – Vertical actions, (*MQI_V*)**	**Masonry quality index – In-plane horizontal actions, (*MQI_{IP}*)**	**Pulse indirect velocity, v_i [m/s]**	**Rebound number, *R***
2	13	Lateral Wall	8.000	6.500	2246.000	50.750
3	16	Bell Tower	5.500	6.000	1521.600	44.250
4	18	Facade	6.500	7.000	2907.200	44.375
5	29	Bell Tower	4.250	4.250	1753.167	30.875
6		Bell Tower	4.250	4.250	1199.667	44.688
7	31	Chapels	2.450	2.450	1697.333	27.813
8		Bell Tower	4.375	4.000	2354.333	23.813
9	34	Lateral Wall	4.025	3.675	2142.000	32.063
10		Transept	4.888	4.463	1717.000	38.313
11	35	Bell Tower	4.000	3.500	1843.000	48.313
12	36	Facade	5.600	5.950	2523.750	32.625
13	39	Lateral Wall	6.750	5.500	2297.000	41.688
14		Apse	5.738	4.675	2300.800	35.750
15		Chapels	5.738	4.675	1587.500	33.875
16	43	Bell Tower	5.000	4.500	1565.000	33.313
17	44	Facade	2.975	2.975	1295.667	35.750
18		Facade	1.750	1.400	2006.000	27.125
19	47	Facade	7.000	8.000	1865.333	55.313
20		Lateral Wall	7.000	8.000	2218.333	56.688
21	48	Facade	3.825	4.250	1280.000	38.500
22		Lateral Wall	3.150	3.500	1256.667	32.875
23		Chapels	3.150	3.500	1281.667	35.938
24	50	Facade	6.500	6.000	1328.000	40.250
25		Lateral Wall	4.550	4.200	1293.667	33.375
26	51	Facade	5.525	5.950	1158.000	38.750
27		Lateral Wall	4.550	4.900	1309.750	31.750

URM type: split stones with good texture						
Specimen #	**Church #**	**Macroblock**	**Masonry quality index – Vertical actions, (MQI_V)**	**Masonry quality index – In-plane horizontal actions, (MQI_{IP})**	**Pulse indirect velocity, v_i [m/s]**	**Rebound number, *R***
28		Apse	2.250	2.500	1238.667	24.188
29	52	Facade	9.000	8.500	2424.333	55.625
30		Lateral Wall	9.000	8.500	2243.333	50.188
31		Nave	9.000	8.500	2785.333	48.563
32		Triumphal Arch	9.000	8.500	2184.000	49.250
33		Bell Tower	8.500	7.500	2332.000	41.188
34	54	Facade	5.000	5.000	1935.333	53.563
35		Lateral Wall	8.000	8.000	3230.250	51.000
36		Apse	8.000	8.000	2220.667	51.625
37		Bell Tower	8.000	8.000	1768.500	47.188
38	55	Apse	1.575	1.875	1927.750	18.313
39		Chapels	3.676	4.375	1079.333	23.875
40	57	Apse	2.125	2.550	505.000	38.625
41		Bell Tower	4.750	5.500	1971.000	40.938

748 *Table B 2 – Collected data for 41 URM specimens for URM type: split stones with good texture.*

URM type: squared stone blocks						
Specimen #	**Church #**	**Macro-block**	**Masonry quality index – Vertical actions, (MQI_V)**	**Masonry quality index – In-plane horizontal actions, (MQI_{IP})**	**Pulse indirect velocity, v_i [m/s]**	**Rebound number, *R***
1	2	Facade	8.500	8.500	2543.000	54.438
2	3	Facade	9.500	9.000	2312.333	48.875
3		Bell Tower	6.800	6.800	1635.333	38.063
4		Nave	9.500	9.000	4479.000	47.594
5		Triumphal Arch	10.000	10.000	2760.000	44.000
6	4	Nave	10.000	10.000	2276.667	40.813
7		Nave	10.000	10.000	5367.667	54.188

URM type: squared stone blocks						
Specimen #	Church #	Macro-block	Masonry quality index – Vertical actions, (MQI_V)	Masonry quality index – In-plane horizontal actions, (MQI_{IP})	Pulse indirect velocity, v_i [m/s]	Rebound number, R
8		Chapels	10.000	10.000	2383.333	45.688
9		Bell Tower	9.500	9.000	6229.500	40.313
10	5	Nave	10.000	10.000	2424.333	45.500
11	5	Transept	10.000	10.000	2539.333	45.000
12	5	Triumphal Arch	10.000	10.000	2635.667	48.438
13	5	Chapels	10.000	10.000	2274.667	45.500
14	6	Facade	8.500	7.500	1399.750	41.125
15	6	Facade	8.500	9.000	1581.000	40.313
16	6	Lateral Wall	7.225	6.375	1921.750	37.125
17	6	Nave	10.000	10.000	4214.750	41.688
18	6	Triumphal Arch	8.500	9.000	2794.000	47.438
19	6	Apse	8.500	9.000	2389.500	43.188
20	6	Bell Tower	5.000	5.000	1407.400	43.313
21	9	Bell Tower	6.800	6.800	1505.500	37.500
22	11	Lateral Wall	9.500	9.500	2617.333	52.250
23	12	Facade	9.500	8.000	3214.000	52.750
24	13	Triumphal Arch	10.000	10.000	1486.667	47.471
25	14	Nave	10.000	10.000	3091.000	42.813
26	14	Triumphal Arch	10.000	10.000	3724.250	45.375
27	14	Bell Tower	8.500	8.500	1811.333	41.063
28	15	Chapels	10.000	10.000	2723.500	49.375
29	15	Bell Tower	8.000	7.000	1285.667	47.875
30	16	Facade	4.900	5.250	1274.750	33.188
31	16	Nave	7.000	7.500	1188.000	47.063
32	16	Nave	10.000	10.000	2898.600	43.938
33	16	Triumphal Arch	10.000	10.000	3635.333	49.250

URM type: squared stone blocks						
Specimen #	**Church #**	**Macro-block**	**Masonry quality index – Vertical actions, (MQI_V)**	**Masonry quality index – In-plane horizontal actions, (MQI_{IP})**	**Pulse indirect velocity, v_i [m/s]**	**Rebound number, *R***
34	17	Nave	10.000	10.000	4670.400	53.500
35		Triumphal Arch	5.000	5.000	1267.333	22.875
36	19	Lateral Wall	6.800	7.225	1252.000	39.813
37		Chapels	8.500	7.000	1441.600	49.375
38	20	Bell Tower	7.225	7.650	1667.333	34.688
39	27	Bell Tower	8.500	7.000	2071.800	40.000
40	28	Bell Tower	6.300	5.250	1984.167	30.250
41	31	Facade	10.000	9.000	3106.600	42.375
42		Nave	10.000	10.000	2924.600	52.500
43	32	Facade	10.000	9.000	3158.000	47.375
44	34	Facade	7.000	7.000	1606.667	34.250
45	35	Facade	9.000	8.000	3711.667	52.313
46	36	Nave	10.000	10.000	2024.000	47.125
47		Chapels	3.825	4.250	1559.000	33.875
48	37	Bell Tower	10.000	9.500	2424.333	46.438
49	38	Facade	9.500	9.000	2299.800	47.000
50		Lateral Wall	9.500	9.000	2227.000	41.375
51		Transept	6.375	5.950	1787.250	39.313
52		Bell Tower	6.650	6.300	2166.333	31.563
53	39	Facade	7.225	7.650	2403.333	34.750
54		Nave	6.650	6.825	1594.600	30.375
55		Triumphal Arch	6.650	6.825	1499.200	32.875
56	40	Facade	9.250	9.000	2842.500	40.938
57		Lateral Wall	9.250	9.500	3102.500	39.813
58		Transept	9.250	9.500	3034.000	41.063
59	57	Facade	9.500	9.500	2084.600	54.500

URM type: squared stone blocks						
Specimen #	**Church #**	**Macro-block**	**Masonry quality index – Vertical actions, (MQI_V)**	**Masonry quality index – In-plane horizontal actions, (MQI_{IP})**	**Pulse indirect velocity, v_i [m/s]**	**Rebound number, R**
60		Lateral Wall	9.500	9.500	1853.250	53.063
61		Chapels	9.500	9.500	2602.667	56.563
62	59	Facade	6.825	5.950	1159.750	28.188
63	60	Facade	8.500	7.500	2167.000	52.813
64		Lateral Wall	7.750	7.000	1873.000	49.000
65	61	Lateral Wall	5.000	5.000	1121.143	48.188
66		Nave	8.500	7.500	1174.667	43.313
67		Facade	8.000	7.000	2908.000	50.813
68	62	Facade	7.000	7.000	1681.000	34.063
69	65	Facade	9.500	9.500	1619.000	53.188
70		Nave	6.500	6.000	1785.667	47.500
71	67	Triumphal Arch	2.550	2.250	1057.333	20.375
72	68	Bell Tower	2.850	2.850	618.667	13.500
73	70	Facade	5.000	5.000	1638.667	23.250
74		Bell Tower	2.400	2.100	1429.333	17.875
75	72	Triumphal Arch	2.850	2.400	1889.000	19.563

Table B 3 – Collected data for 75 URM specimens for URM type: squared stone blocks.

URM type: Fired clay bricks with lime mortar						
Specimen #	**Church #**	**Macro-block**	**Masonry quality index – Vertical actions, (MQI_V)**	**Masonry quality index – In-plane horizontal actions, (MQI_{IP})**	**Pulse indirect velocity, v_i [m/s]**	**Rebound number, R**
1	18	Facade	5.100	4.675	1160.000	35.813
2		Lateral Wall	6.125	5.600	1127.600	34.688
3	19	Lateral Wall	6.800	7.225	1252.000	39.813
4		Apse	5.600	5.950	1010.600	34.643
5		Bell Tower	5.950	6.800	1092.667	38.063

URM type: Fired clay bricks with lime mortar						
Specimen #	Church #	Macro-block	Masonry quality index – Vertical actions, (MQI_V)	Masonry quality index – In-plane horizontal actions, (MQI_{IP})	Pulse indirect velocity, v_i [m/s]	Rebound number, *R*
6	21	Bell Tower	6.125	6.300	1277.333	33.625
7	25	Lateral Wall	5.600	5.950	822.600	34.417
8		Bell Tower	6.800	6.375	1646.000	37.200
9	26	Bell Tower	2.800	2.800	1469.000	33.813
10	28	Bell Tower	5.250	5.250	1321.600	28.813
11	30	Bell Tower	5.775	5.250	849.200	33.176
12	32	Facade	6.650	6.650	1278.333	32.500
13	36	Lateral Wall	3.150	2.275	1831.333	34.313
14	37	Facade	5.250	5.250	1068.667	29.875
15		Lateral Wall	6.800	7.225	1530.000	36.813
16		Transept	8.000	8.500	1343.333	41.750
17	41	Facade	8.075	8.075	2196.000	39.438
18	43	Facade	9.500	9.500	2211.000	41.063
19	45	Facade	8.075	8.075	1530.000	37.500
20		Lateral Wall	9.500	9.500	1917.000	39.063
21		Bell Tower	6.800	7.225	2046.667	36.188
22	46	Facade	8.075	8.075	1530.167	37.875
23		Lateral Wall	6.650	6.650	1393.500	32.469
24		Lateral Wall	6.650	6.650	1739.833	34.344
25	49	Facade	6.375	6.375	1153.667	34.938
26		Lateral Wall	6.375	6.375	1277.667	35.125
27		Chapels	6.375	6.375	1533.000	36.750
28		Bell Tower	8.075	8.075	1694.000	35.875
29	52	Apse	6.300	5.950	1292.000	32.000
30		Chapels	9.000	8.500	1400.667	44.063
31	53	Facade	9.500	9.500	2040.000	39.188

URM type: Fired clay bricks with lime mortar						
Specimen #	**Church #**	**Macro-block**	**Masonry quality index – Vertical actions, (*MQI_V*)**	**Masonry quality index – In-plane horizontal actions, (*MQI_{IP}*)**	**Pulse indirect velocity, v_i [m/s]**	**Rebound number, *R***
32	58	Facade	8.000	7.500	2362.000	43.250
33		Lateral Wall	6.800	6.375	1303.000	39.250
34	59	Facade	6.475	5.600	1415.667	33.438

Table B 4 – Collected data for 34 URM specimens for URM type: solid fired clay bricks with lime mortar.